Chapter 7

Advanced Hybrid Materials Based on Titanium Dioxide for Environmental and Electrochemical Applications

Katarzyna Siwińska-Stefańska and
Teofil Jesionowski

Additional information is available at the end of the chapter

http://dx.doi.org/10.5772/intechopen.69357

Abstract

Constant technological progress, as well as the pursuit of "friendly" technologies, leads to intensive work on the development of a new generation of advanced products with strictly defined, unique physicochemical properties dedicated to specific applications. This group of materials includes hybrids based on titanium dioxide and its derivatives, characterised with specific, well-defined physicochemical and structural properties, chiefly determined during their synthesis. Different properties of titania nanoparticles depend on their morphology, crystallite size, and crystalline structure. Nanocrystalline titanium dioxide can be synthesised via different methods, among which chemical precipitation, microemulsion method (inversed micelles), sol-gel process and hydrothermal crystallisation are the most important ones. That is why, a crucial part of the following chapter will be paid to characterisation of synthesis routes used for titanium dioxide and titania-based hybrid production. Furthermore, application of TiO_2-based materials, including mixed oxide systems as well as graphene oxide–based hybrids, in electrochemical (electrode material) and environmental (photocatalysis) aspects, will be described in detail.

Keywords: titanium dioxide, TiO_2-based hybrid materials, advanced material synthesis, photocatalyst, electrode material

1. Introduction

Titanium dioxide, commonly known as titanium white, is in normal conditions a colourless crystalline solid. It is non-toxic, non-hygroscopic, inflammable and non-volatile. It shows high chemical stability: it does not dissolve in water, organic solvents, acids (except for concentrated hydrofluoric acid and sulphuric acid) or alkalis. It is amphoteric, but more acidic

than basic. Titanium dioxide is thermally stable: it loses oxygen only at a temperature of a few hundred degrees Celsius and under the influence of reducing agents (carbon, magnesium, hydrogen and halogens). Its melting point is 1825°C, while its boiling point is close to 2500°C. Above 400°C, a reversible change in colour to yellow takes place as a result of thermal expansion of the crystalline lattice. Above 1000°C, the oxide forms of titanium are formed, characterised by a lower content of oxygen than in TiO_2, an undesirable colour change takes place and the electrical conductivity changes. Titanium dioxide does not show activity towards living organisms [1–4].

Titanium dioxide occurs in nature in three polymorphous varieties: tetragonal rutile, anatase and rhombic brookite. Anatase and rutile are of practical importance and are commonly used in many applications, while brookite is not used because of the instability of its structure [4–6].

The rapidly developing technologies for obtaining new functional materials based on titania are an especially important topic for both theoretical study and practical application. The continually growing requirements of different technologies require new directions to be sought in order to obtain materials with precisely designed physicochemical and structural properties. Hybrid systems based on TiO_2 constitute a new group of compounds exhibiting strictly designed physicochemical properties resulting from the effects of combining the characteristic behaviours of the individual compounds from which they are made. The presence of a foreign element in the matrix of pure titania can greatly affect the structural, textural, acid/base and catalytic properties [7]. The textural properties of the hybrid materials, such as pore size distribution, surface area, etc., are strongly dependent upon the conditions of synthesis, including the nature and composition of the precursors, solvent, complexing/templating agent, hydrolysis and calcination conditions [8]. Research into the production and potential applications of new functional materials based on titanium dioxide is only possible when the final materials have a strictly defined dispersive character, crystalline structure, morphology and porous structure [9–13].

2. Synthesis of titanium dioxide and its derivatives

The synthesis of titanium dioxide is one of the major research areas in 'green chemistry'. Titania is a chemically inert, thermally stable, insoluble, biocompatible, non-toxic material, and an excellent absorber of destructive UV radiation. Because of these properties, titanium dioxide and its derivatives have for some time enjoyed a great and still growing popularity in many applications; see **Figure 1** [1–4].

On an industrial scale, titanium dioxide pigments are obtained by two methods (see **Figure 2**) whose names refer to the substrate salts used:

- the sulphate method, in which TiO_2 is precipitated from a solution of ilmenite ore by concentrated sulphuric acid, leading to both rutile and anatase;
- the chloride method, in which titanium dioxide is obtained by oxidation of titanium tetrachloride ($TiCl_4$) obtained by reduction and chlorination of ilmenite ore; this method leads only to rutile.

http://dx.doi.org/10.5772/intechopen.69357

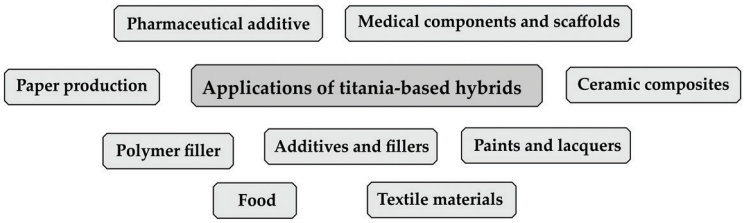

Figure 1. Applications of titania-based materials.

The use of the chloride process is on the increase. It is estimated that over half of the world's titanium dioxide is produced in this way. Although this process requires higher quality, previously enriched ore and more complex technology, it produces much less waste than the sulphate method, and the cost of production is also lower [1].

The properties of TiO_2 are determined by the morphology of its particles, the size of its crystals and its crystalline structure, which depend on the choice of method for its synthesis and final heat treatment [14]. Nanocrystalline TiO_2 particles are usually obtained by crystallisation (chemical precipitation) [15], the microemulsion method (reverse micelles) [16], the sol-gel method [17–21] or hydrothermal crystallisation [22–26]; see **Figure 2**. Each of these methods has its advantages and drawbacks, but a feature of all of them is the ability to obtain materials with strictly defined properties (**Table 1**).

Additionally, **Table 2** presents a comprehensive review of different methods of synthesis of titania-based materials.

2.1. Chemical precipitation

Co-precipitation is a wet chemical method and is one of the oldest methods for obtaining nanometric materials. The most common precursors used in this method are salts: nitrates,

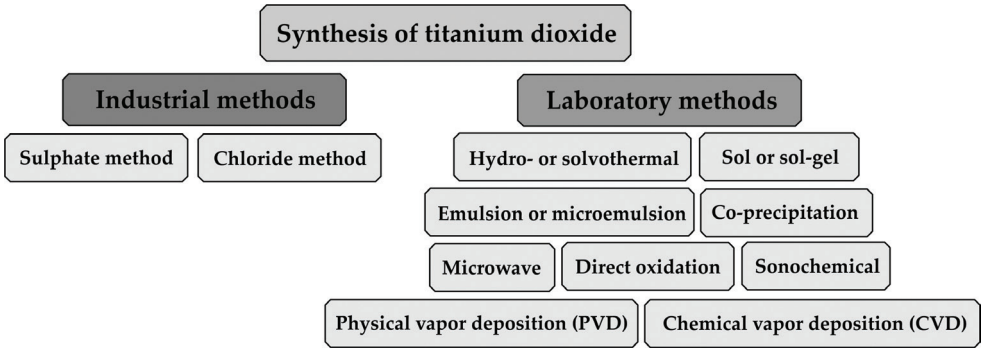

Figure 2. Synthesis of titanium dioxide.

Method	Advantages	Disadvantages
Sulphate method	Ability to control the crystalline structure; possibility of using low-quality ore	Susceptibility to agglomeration of particles; high energy costs; large quantities of waste produced and requiring disposal
Chloride method	High-quality products (including for medical applications); defined morphological structure and high degree of particle dispersion	Need to use high-quality substrates; production of only the rutile form, advanced technology; hazardous reaction environment, toxicity; danger of uncontrolled emission of chlorine gas
Co-precipitation method	Homogeneous mixing of reactant precipitates reduces the reaction temperature; a simple direct process for the synthesis of fine material powders which are highly reactive in low-temperature sintering	Not suitable for the preparation of a highly pure, stoichiometrically accurate phase; this method does not work well if the reactants have very different solubilities and precipitation rates; it does not meet universal experimental conditions for the synthesis of various types of metal oxides
Sol-gel route	Low temperature processing and consolidation is possible; smaller particle size and morphological control in powder synthesis; sintering at low temperature also possible; better homogeneity and phase purity than in traditional ceramic methods	Raw materials for this process are expensive (in the case of metal alkoxides) compared with mineral-based metal ion sources; products have high carbon content when organic reagents are used in the preparative steps and this inhibits densification during sintering; since several steps are involved, close monitoring of the process is needed
Hydrothermal route	Powders are formed directly from solution; it is possible to control particle size and shapes by using different starting materials and hydrothermal conditions; the resulting powders are highly reactive, which aid low-temperature sintering	Prior knowledge on the solubility of the starting materials is required; hydrothermal slurries are potentially corrosive; accidental explosion of the high-pressure vessel cannot be ruled out
Solvothermal method	An energy-efficient, environmentally friendly process; high-purity products can be synthesised; metastable and new phases can be accessed; simplified and precise control of the size, shape distribution, and crystallinity of the end product can be achieved via the adjustment of parameters such as reaction temperatures and time, the types of solvents, surfactants and precursors	The need for expensive autoclaves; safety issues during the reaction process; impossibility of observing the reaction process ("black box")

Table 1. Advantages and disadvantages of the most commonly used methods for the synthesis of titanium dioxide.

chlorates or chlorides, which dissolve in an appropriate solvent. Aqueous solutions are used most commonly, but the use of organic solvents is also possible. The precipitation reaction must be initiated; this may be done by changing the pH, concentration or temperature. Another way of starting the precipitation reaction is to carry out a reaction of hydrolysis, oxidation, reduction or complexation. Usually a base (potassium or sodium hydroxide) is added to the system containing the precursors of the oxide. The precipitation reaction itself involves reduction of the metal cation, and formation of a precipitate requires that the system reach saturation point. The precipitation method consists of three stages: nucleation, growth and agglomeration. To begin with, small crystallites are formed (nucleation), which over

Product	Starting materials	Conditions of synthesis	Properties of obtained material	Potential application	Ref.
Co-precipitation method					
TiO_2	$TiCl_4$, HCl, H_2O_2, $NH_3{\cdot}H_2O$	Reaction: ice-water bath, then 10°C, next 50°C, Drying: 60°C, Calcination: 500°C for 2 h	Anatase and rutile structure	Photodegradation of helianthine	[29]
TiO_2	$Ti(OCH(CH_3)_2)_4$ (TTIP), C_3H_7OH, polyvinyl pyrrolidone (PVP)	Reflux: 2 h, Drying: 80°C for one day, Calcination: 800°C	Rutile structure, spherical shape of 10 nm in diameter	–	[30]
TiO_2/SnO_2	$TiCl_4$, $SnCl_4{\cdot}5H_2O$, $CO(NH_2)_2$	Reaction: room temperature, after adding $CO(NH_2)_2$—80°C for 8 h, ageing: room temperature for 24 h, drying: 60°C calcination: 550°C for 4 h	Rutile structure, BET surface area: 82 m^2/g, aggregated particles with a different size distribution, crystallite size: 17.4 nm	Degradation of methyl blue (MB)—90%	[31]
TiO_2/CeO_2 and TiO_2/SnO_2	$Ce(NO_3)_3{\cdot}6H_2O$, $SnCl_4{\cdot}5H_2O$, $Ti(SO_4)_2$, $NH_3{\cdot}H_2O$	Reaction: room temperature, 3 h, pH = 10 ageing: 48 h, drying: 105°C, 12 h, calcination: 500°C for 6 h	BET surface area: TiO_2/CeO_2 = 108 m^2/g, TiO_2/SnO_2 = 59 m^2/g, $TiO_2/CeO_2/SnO_2$ = 139 m^2/g, crystalline structure: TiO_2/CeO_2—anatase, TiO_2/SnO_2—rutile, $TiO_2/CeO_2/SnO_2$—amorphous	Reduction of NO with NH_3	[32]
TiO_2/ZrO_2	$TiCl_4$, $ZrOCl_2{\cdot}8H_2O$, $NH_3{\cdot}H_2O$, HCl	Reaction time: 3 h, ageing: 24 h, drying: 110°C (overnight) calcination: 500°C for 5 h	Amorphous structure, BET surface area: 234 m^2/g	Reduction of NO by NH_3	[33]
Sol-gel method					
TiO_2	$Ti(OC(CH_3)_3)_4$ (TBOT), HCl, CH_3OH, C_2H_5OH, CH_3COOH, F-127 (triblock copolymer)	Reaction time: 60 min, drying: 65°C, ageing: 24 h, calcination: 400, 500, 600, 700 and 800°C in air for 4 h	Anatase and rutile structure, BET surface area from 165 m^2/g (500°C) to 15 m^2/g (800°C) nanoparticles diameter: 10–15 nm (500°C), 50–75 nm (800°C), agglomerates: 1–3 μm (500°C), 1–5 μm (800°C)	Photodegradation of imazapyr (98%) and phenol (95%)	[54]

Product	Starting materials	Conditions of synthesis	Properties of obtained material	Potential application	Ref.
TiO_2	$Ti(OCH(CH_3)_2)_4$ (TTIP), C_3H_7OH, NaOH, HNO_3	Reaction: 80°C (5 h), then cooling to room temperature, ageing: 25°C for 24 h, drying: 100°C for 12 h, calcination: 200, 600 and 800°C for 2 h	Anatase-brookite (calcination at 200°C), anatase-brookite-rutile (calcination at 600 and 800°C), irregular clusters composed of spherical nanomeric primary particles (200 nm—pH = 2, 400 nm—pH = 9), BET surface area: pH = 2—calcination at: 200°C—186 m^2/g, 600°C—48 m^2/g, pH = 4—calcination at: 200°C—109 m^2/g, 600°C—42 m^2/g	Photodegradation of methylene blue (MB)—98%—samples calcined at 200 or 600°C by pH = 2	[55]
TiO_2/SiO_2	$Si(OC_2H_5)_4$ (TEOS), C_2H_5OH, HCl, $Ti(OCH(CH_3)_2)_4$ (TTIP)	Reaction: room temperature, ageing: room temperature for 72 h, drying: 80°C, calcination: 1000°C for 2 h	Anatase structure (400°C), rutile with a small amount of anatase (800°C), rutile (1000°C)	–	[57]
TiO_2/ZrO_2	$Ti(OC(CH_3)_3)_4$ (TBOT), HNO_3, C_2H_5OH, Pluronic P123 and Macrogol 20000 (triblock copolymers), $ZrOCl_2{\cdot}8H_2O$	Reaction: room temperature, after adding Zr precursor—80°C, ageing: room temperature for 24 h, drying: room temperature in air, calcination: 800°C for 5 h	Anatase structure, BET surface area: 149 m^2/g	Photodegradation of Rhodamine B (RhB)—90%	[59]
TiO_2, TiO_2/ZrO_2	$TiOCl_2$, $ZrO(NO_3)_2$, NaOH, cetyltrimethylammonium bromide (CTAB), C_2H_5OH	Reaction: room temperature, ageing: 80°C for 4 h, drying: 100°C for 6 h, calcination: 600-900°C for 2 h	Irregular spherical agglomerates, crystalline structure: 600°C—anatase TiO_2 and tetragonal ZrO_2 crystals, 800°C—rutile and anatase TiO_2 and tetragonal ZrO_2 crystals, 900°C—rutile TiO_2 and tetragonal and monoclinic ZrO_2 crystals, BET surface area: TT-600—88 m^2/g, ZT8-600—70 m^2/g, ZT14-600—62 m^2/g, ZT22-600—63 m^2/g, ZT32-600—61 m^2/g	Photodecolorization of the MB—sample ZT8-600—94.1%	[60]
ZrO_2/Al_2O_3 and TiO_2/Al_2O_3	2,4-Pentanedione, n-butanol, alkoxides of the respective metals	Reaction: room temperature, then 70°C drying, calcination: 500°C	Amorphous structure of TiO_2/Al_2O_3, crystalline size: TiO_2/Al_2O_3—4.9 nm, ZrO_2/Al_2O_3—4.1 nm, BET surface area: TiO_2/Al_2O_3—320 m^2/g, ZrO_2/Al_2O_3—200 m^2/g	Ethanol conversion: TiO_2/Al_2O_3—99%, ZrO_2/Al_2O_3—47%	[61]

Product	Starting materials	Conditions of synthesis	Properties of obtained material	Potential application	Ref.
TiO_2/ZrO_2	$Zr(OCH_2CH_2CH_3)_4$, $Ti(OCH_2CH_2CH_3)_4$, C_3H_7OH, $NH_3{\cdot}H_2O$	Reaction: 18°C, pH = 9, then 27°C, refluxe: 1 h, ageing: 24 h, heating: 100°C for 24 h, calcination: 550 and 700°C for 5 h	Crystalline structure: anatase (66 wt.%), rutile (19 wt.%) and orthorhombic (15 wt.%) srilankite type—sample TiZr13 calcined at 700°C, amorphous—sample TiZr37 calcined at 550°C, BET surface area: sample TiZr37 calcined at 550°C—172 m^2/g	–	[62]
Hydrothermal method					
TiO_2	$Ti(OCH(CH_3)_2)_4$ (TTIP), C_2H_5OH, HNO_3	pH = 0.7, hydrothermal treatment—240°C for 4 h, drying: room temperature	Anatase and brookite structure, size of particles—21–23 nm BET surface area: 190 m^2/g (7 nm), 124 m^2/g (15 nm), 75 m^2/g (24 nm)	Decomposition of propan-2-ol to CO_2 (98%)	[65]
TiO_2	Anatase TiO_2, NaOH	Hydrothermal treatment—200°C for 24 h, drying: 70°C for 6 h	Anatase and brookite structure, TiO_2 nanowires	–	[66]
TiO_2/ZrO_2	$ZrOCl_2{\cdot}8H_2O$, $TiCl_4$, $TiCl_4$, $NH_3{\cdot}H_2O$	Hydrothermal treatment—220°C for 4 h, 25 bar drying: 120°C calcination: 500°C for 10 h	Amorphous structure, BET surface area: 209 m^2/g	–	[67]
TiO_2/ZrO_2	$TiOSO_4$, $ZrCl_4$	Hydrothermal treatment—200–240°C for 48 h, drying: 60°C calcination: 400–1000°C for 1 h	Anatase structure	Photodecolorization of the MB	[68]
Solvothermal method					
TiO_2	Polyethyleneimine (PEI), C_2H_5OH, $Ti(OC(CH_3)_3)_4$ (TBOT)	Mixing: 5 h, thermal treatment—180°C for 24 h, drying: 60°C, 6 h, calcination: 400°C for 2 h	Anatase structure, crystalline size: 12.1 nm, sample after calcination: anatase (82.3%) and rutile (17.7%) structure, quasi-spherical nanostructures with diameters of ca. 100–200 nm, BET surface area: 118 m^2/g	Photodegradation of methyl orange (MO)—74% and phenol—82%	[71]

Product	Starting materials	Conditions of synthesis	Properties of obtained material	Potential application	Ref.
TiO_2	HCl, TiF_4, C_3H_7OH, HF	Thermal treatment—180°C for 5.5–44 h, drying: in vacuum overnight, calcination: 600°C for 90 min	Anatase structure	–	[72]
TiO_2/SiO_2 and TiO_2/ZrO_2	Titanium(IV) n-butoxide, tetraethylorthosilicate, zirconium(IV) n-butoxide, toluene	Thermal treatment—300°C	Anatase structure, crystallite size from 11.0 to 9.0 nm, BET surface area: TiO_2/SiO_2—from 133 to 156 m^2/g, TiO_2/ZrO_2—from 95 to 106 m^2/g	Conversion of ethylene TiO_2/SiO_2—from 22.1 to 32.4%, TiO_2/ZrO_2—from 22.2 to 39.5%	[74]

Table 2. Synthesis of titania-based materials via different method.

time become more thermodynamically stable and larger (the growth stage); then as more time elapses, the permanent crystallites combine into persistent agglomerate forms (agglomeration). The properties of the final material are strongly influenced by the initial nucleation stage. An important part is also played by the particle agglomeration stage, which determines the morphological properties of the system [27, 28]. To obtain the final product, the dried precipitate is subjected to thermal treatment at the required temperature in an appropriate atmosphere.

Liu et al. [29] prepared titanium dioxide by five different methods: co-precipitation, the sol-gel route, hydrolysis, the hydrothermal method and sluggish precipitation. They investigated how the method used affected the physicochemical properties of the resulting TiO_2. Synthesis of TiO_2 by the co-precipitation method was carried out using titanium tetrachloride, hydrochloric acid, hydrogen peroxide and ammonia. Titanium tetrachloride as a precursor of TiO_2 was added to hydrochloric acid and deionised water. The resulting mixture was maintained at a temperature below 10°C, and hydrogen peroxide was added. Finally, ammonia was added to the solution (pH = 10). The resulting sample was calcined at 500°C for 2 h. XRD analysis showed that this procedure of TiO_2 synthesis leads to a mixture of anatase and rutile phases with anatase predominant. The material synthesised by the co-precipitation method also demonstrated with good photocatalytic activity in the decomposition of helianthine (with absorbency equal to 0.25 and transmission equal to 60.0).

Muhamed Shajudheen et al. [30] synthesised titanium dioxide using titanium tetraisopropoxide as a Ti precursor and poly(vinyl pyrrolidone) (PVP) as a capping agent. To a mixture consisting of titanium tetraisopropoxide and propan-2-ol, PVP and then water were added. The resulting white precipitate was refluxed for 2 h and then stirred continuously for 1 day, followed by calcination at 800°C. The proposed co-precipitation method allows synthesis of the rutile phase of titania in a single-step process without impurities and other phases, as was confirmed by XRD and Raman spectroscopy.

To alter the physicochemical properties of titanium dioxide, Huang et al. [31] prepared SnO_2/TiO_2 catalysts using five different preparation methods: the sol-gel method (SGM), the sol-hydrothermal method (SHM), the co-precipitation method (CM), a co-precipitation-hydrothermal method (CHM) and the hydrothermal method (HM). They determined the impact of the methodology for obtaining SnO_2/TiO_2 systems on the structure, chemical composition, particle sizes, specific areas, pore size distribution and energy band structure. The synthesis of SnO_2/TiO_2 by the co-precipitation method was carried out using $TiCl_4$ and $SnCl_4 \cdot 5H_2O$, which were dissolved in deionised water. In the next step, the obtained solution was added to an aqueous solution of urea. At this stage of the synthesis, the reaction was carried out at a temperature of 80°C for 8 h. At the final stage, the resulting material was calcined at 550°C for 4 h. XRD analysis of the sample obtained by the co-precipitation method revealed the presence of diffraction peaks indicating a pure rutile structure. Moreover, peaks corresponding to SnO_2 were not present in the pattern. This may indicate that the Sn^{4+} ion was successfully incorporated into the crystal lattice sites of the titania to form uniform SnO_2/TiO_2 solid solutions, or that the reflection bands attributed to SnO_2 overlapped with the crystalline plane of TiO_2. Moreover, the synthesised sample demonstrated

good photocatalytic activity in the degradation of methyl blue. It was shown that the structure, crystallinity, dispersity, light adsorption properties and photocatalytic performance of SnO_2/TiO_2 photocatalysts are critically dependent on the preparation method.

Another example of the use of a precipitation method to obtain TiO_2/CeO_2 and TiO_2/SnO_2 systems is reported by Yu et al. [32]. As precursors of titanium dioxide, cerium oxide and tin oxide, they used titanium(IV) sulphate(VI), cerium(III) nitrate(V) hexahydrate and tin chloride pentahydrate. The precipitating agent was an aqueous solution of ammonia. Aqueous solutions of the oxide precursors were stirred for 1 h until the components dissolved completely, and then, ammonia solution was added to the reaction mixture. The process was carried out at room temperature, and the pH of the reaction mixture was maintained at 10. After all solutions had been added in the appropriate quantities, the system was stirred for a further 3 h. The material was then subjected to an ageing process for 48 h. The resulting precipitate was dried at 105°C for 12 h and then calcined at 500°C for 6 h. Physicochemical analysis revealed specific surface areas of 108 and 59 m^2/g respectively for the TiO_2/CeO_2 and TiO_2/SnO_2 systems. X-ray analysis showed the TiO_2/CeO_2 system to have an anatase crystalline structure, while for TiO_2/SnO_2, the diffractogram contained peaks corresponding to rutile. In both cases, the crystalline structure of cerium or tin oxide was not observed. The catalytic properties of the systems were also investigated; they demonstrated excellent performance in the reduction of nitrogen oxides.

Zhang et al. [33] synthesised TiO_2/ZrO_2 mixed oxide (with molar ratio = 1:1) by a co-precipitation method from $TiCl_4$ and $ZrOCl_2$ aqueous solutions, which were hydrolysed with ammonium hydroxide. The precursors of Ti and Zr were dissolved in deionised water, and then, HCl was added. Ammonia was added to the solution until pH = 10. Finally, the samples were dried at 110°C and then calcined at 500°C for 5 h. The Ti/Zr mixed oxide synthesised by a co-precipitation method was found to have a high specific surface area of 234 m^2/g, which is linked to the amorphous structure of the material. No diffraction peaks characteristic of TiO_2 or ZrO_2 were detected in the obtained sample. Moreover, the TiO_2/ZrO_2 mixed oxide exhibited good catalytic activity for the selective catalytic reduction of NO by NH_3.

2.2. Sol-gel method

The sol-gel route is a wet chemical method and is a multi-step procedure involving both chemical and physical processes such as hydrolysis, polymerisation, gelation, drying, dehydration and densification. In a typical sol-gel process, a colloidal suspension or sol is obtained as a result of hydrolysis and polycondensation of precursors, which are usually inorganic metal salts or organometallic compounds such as metal alkoxides. Polycondensation and the loss of solvent lead to a transformation from the fluid sol to the solid gel phase [34–38]. The sol-gel method is based on hydrolysis and condensation of metal alkoxides or metal salts [39]. The process involves the reaction of a metal chloride with metal alkoxide or an organic ether, which is an oxygen donor, according to Eqs. (1) and (2):

$$MCl_n + M(OR)_n \rightarrow 2MO_{n/2} + n\mathrm{RCl} \quad (1)$$

http://dx.doi.org/10.5772/intechopen.69357

$$MCl_n + (n/2)ROR \rightarrow MO_{n/2} + nRCl \quad (2)$$

In these reactions, the formation of ≡M–O–M≡ type bonds is favoured by the condensation between ≡M–Cl and ≡M–OR, according to the reaction (3):

$$\equiv M–Cl + \equiv M–O–R \rightarrow \equiv M–O–M\equiv + R–Cl \quad (3)$$

In the reaction with ether (4), an alkoxide is formed as a result of a reaction of alcoholysis with ≡M–Cl:

$$\equiv M–Cl + R–OR \rightarrow \equiv M–OR + R–Cl \quad (4)$$

These reactions run slowly, and usually, the formation of inorganic oxide is favoured by elevated temperature in the range 80–150°C. The main reaction (5) between metal chloride and metal alkoxide takes place at room temperature and leads to a solution of metal chloroisopropoxide:

$$\equiv M–Cl + \equiv M–OR \rightarrow \equiv M–OR\equiv + \equiv M–Cl \quad (5)$$

The properties of materials obtained by the sol-gel method depend on such factors as pH, the presence of admixtures of other substances, the volume ratio of water to precursor, and the rate of stirring of the system. The pH also influences the size and shape of pores [38].

Advanced materials in a wide variety of forms, such as spherical or ultrafine shaped powders, fibres, thin film coatings, dense or porous materials including high-purity inorganic oxides, and hybrid (inorganic-organic) materials can be synthesised using the sol-gel method [40–43]. The sol-gel process is a useful synthetic method for the preparation of amorphous as well as structurally ordered products [44–49]. It is of particular interest because it gives very good compositional and morphological control over the product's properties, such as specific surface area, nanoparticle size and degree of aggregation. The precipitates or gels obtained by sol-gel processing are typically amorphous, exhibiting a fairly high specific surface area and are in some cases even (meso)porous. A transition from the amorphous to the crystalline phase is typically induced by thermal treatment at temperatures higher than 300°C, leading in most cases to a deterioration of the pore system and an increase in the particle size, associated with a decrease in the specific surface area. In sol-gel processing, for better control of the hydrolysis and condensation process, many different modifiers of alkoxide precursors can be used, including acetylacetone [50–52], acetic acid [50, 53] and other complex ligands.

Mesoporous TiO_2 nanocrystals were synthesised by Faycal Atitar et al. [54] using the sol-gel method in the presence of triblock copolymer as the structure directing agent. In the typical synthesis, triblock copolymer was first dissolved in ethanol, and the resulting mixture was added to CH_3COOH and HCl. Next, $Ti(OC(CH_3)_3)_4$ (TBOT) was added to the mixture. The resulting TiO_2 nanocrystals were calcined at different temperatures (400, 500, 600, 700 and 800°C for 4 h) to demonstrate how their structural properties such as crystallite phases,

morphology and mesoporosity affect the photocatalytic performance. X-ray analysis showed the samples to have a crystalline structure. The samples calcined at 400 and 500°C revealed the presence of anatase, but as the calcination temperature increased, the contribution of the anatase crystalline structure decreased in favour of rutile. All the synthesised materials were shown to be photocatalytically active, and the photocatalytic activity of mesoporous TiO_2 was strongly dependent on the final thermal treatment. The sample calcined at 500°C demonstrated higher activity in the decomposition of imazapyr (98%) and phenol (95%) compared with the commercially available Aeroxide TiO_2 (P-25). Based on the results obtained, the authors concluded that mesoporous titanium dioxide T-500 (calcined at 500°C) is an efficient material for the removal of organic pollutants from water.

The sol-gel route was also used by Mutuma et al. to obtain titanium dioxide [55]. The precursor used was titanium tetraisopropoxide (TTIP), which was dissolved in propan-2-ol and deionised water. The reaction mixture was heated to 80°C and maintained at that temperature for 5 h, after which it was cooled to room temperature. It was determined how the pH of the reaction system affected the physicochemical properties of the products. The pH was controlled by adding a precipitating agent in the form of a solution of sodium hydroxide or nitric(V) acid. The process was carried out at pH values of 2, 4, 7 and 9. The resultant systems were left to gel at room temperature for 24 h. The products were dried at 100°C for 12 h and then calcined at temperatures of 200, 600 and 800°C for 2 h. It was also determined how the process conditions influenced the crystalline and porous structures of the synthesised materials, which have a significant effect on their photocatalytic properties. X-ray analysis showed that titanium dioxide that had not undergone calcination had an anatase structure. Calcination at 200°C led to the appearance of brookite, although the intensity of the band corresponding to that crystallographic form decreased as the calcination temperature increased. When the calcination temperature increases to 800oC, bands corresponding to rutile appeared, indicating a transformation of anatase to rutile. In photocatalytic tests, the materials containing anatase-brookite (calcined at 200°C) or anatase-brookite-rutile (600 and 800°C) exhibited better photocatalytic properties than an anatase-rutile system (800°C). It was also found that the specific surface area of the products depends strongly on the pH of the reaction system. As the pH increased, the surface area of the synthesised materials decreased, irrespective of the calcination temperature. The experiments showed the systems with mixed crystalline structure to be an excellent photocatalytic material in the decomposition of non-biodegradable organic pollutants, for example from the textile industry.

Titanium dioxide powders were also prepared via the sol-gel method by Siwińska-Stefańska [56]. It was investigated how the conditions of preparation (addition of catalyst and chelating agent, temperature of calcination) affect the microstructural evolution, porous structure parameters and photocatalytic capability of the resulting TiO_2 powders. The results of dispersive analysis showed that an increase in the amount of catalyst used in the process of obtaining titanium dioxide results in an increase in particle diameter. Moreover, the diameter of particles tended to decrease with a decreasing quantity of chelating agent. The addition of chelating agent also caused significant changes in the crystalline structure and porous structure parameters of the resulting samples. The TiO_2 systems prepared by the sol-gel method with or without the

addition of chelating agent exhibited relatively high photocatalytic activity in the decomposition of C.I. Basic Blue 9.

In a report by Italian researchers [57], the sol-gel method was used to obtain an SiO_2/TiO_2 system. The precursors of the dioxides were respectively TEOS and TTIP. First, TEOS was mixed with an organic solvent (ethanol) in the molar ratio TEOS:ethanol:water = 1:2:1. Hydrochloric acid was added to the mixture to maintain a pH of 1. After stirring for 6 h, TTIP was added to the system. The resulting sol was matured for 3 days to obtain a gel, which was then dried at room temperature for 7 days. The resulting materials then underwent calcination at temperatures of 600 and 800°C for 2 h. Detailed physicochemical analysis confirmed that the product consisted of titanium dioxide in rutile form and silicon dioxide. X-ray analysis showed that the system that had not been calcined had an amorphous structure, while calcination caused the formation of a crystalline structure. Calcination at 600°C leads to anatase, but when a temperature of 800°C is used, rutile appears. TEM microscopic images revealed a tendency for the agglomeration of particles in the samples. Variation in the molar ratio of the oxides was found not to have a significant effect on the morphology of the oxide system.

Siwińska-Stefańska et al. [58] reported the preparation of nano- and microstructured TiO_2 doped with Fe and Co by the sol-gel method and determined the effect of doping on the physicochemical properties of TiO_2. The doped materials were found to contain particles of smaller diameter and lower homogeneity than pure TiO_2. XRD analysis revealed that the addition of iron or cobalt to the titania preparation process has a significant effect on crystalline structure formation.

Fan et al. [59] prepared a mesoporous TiO_2/ZrO_2 nanocomposite from titanium tetrabutoxide, $ZrOCl_2 \cdot 8H_2O$, Pluronic P123 and Macrogol 20000 as double templates utilising the sol-gel method. In typical synthesis, to a solution of titanium tetrabutoxide and nitric acid, ethanol, Pluronic P123 and Macrogol 20000 were added. The resulting material was calcined for 5 h at 800°C. The structures and physicochemical properties of the products were determined by X-ray diffraction (XRD), Raman scattering studies and N_2 adsorption/desorption. The results proved that the use of double templates retarded the crystal phase transformation from anatase to rutile, and the obtained materials showed high thermal stability. Moreover, photocatalytic tests confirmed that the sample prepared with double templates exhibited higher photocatalytic activity in the decomposition of Rhodamine B (92%) than samples prepared with a single template (90 and 91%).

In another study, Shao et al. [60] obtained pure TiO_2 and TiO_2/ZrO_2 system using the sol-gel method. The crystalline structure and particle shape and size were found to be strongly dependent on the calcination temperature and on the ratio of Zr to Ti. XRD analysis showed the crystalline structure of the synthesised materials to be significantly affected by the conditions of calcination. As the content of ZrO_2 increased, the intensity of the bands corresponding to anatase (TiO_2) decreased in favour of those corresponding to tetragonal ZrO_2. When samples were treated at 800°C, the transformation of anatase to rutile was favoured, although a high content of zirconium dioxide retarded that effect. Further increase in the calcination temperature led to the transformation of tetragonal ZrO_2 to monoclinic.

Kraleva and Ehrich [61] obtained the oxide systems ZrO_2/Al_2O_3 and TiO_2/Al_2O_3 by the sol-gel route. They used 2,4-pentanedione as complexing agent and n-butoxide as solvent. The precursors of the component oxides were the alkoxides of the respective metals. The molar ratio of the precursors was 1:1. An appropriate quantity of the precursors was dissolved in the solvent, and the reaction system was stirred continuously for approximately 30 min. A complexing agent with a pH of 8 was then added, and the mixture was stirred for another 5 min. It was then heated to 70°C with the pH maintained at 8 for 10 min. Next, hydrolysis was performed by adding deionised water dropwise to the reaction mixture and stirring for 1 h. The sample was then left to cool at room temperature for 12 h, and then, the solvent was removed by pressure evaporation at 110°C. After drying, the system was calcined at 500°C. The resulting systems had high specific surface area (320 and 200 m^2/g respectively for TiO_2/Al_2O_3 and ZrO_2/Al_2O_3). The materials differed significantly in terms of crystallinity: the system containing titanium dioxide with aluminium oxide was completely amorphous, while that of zirconium dioxide with aluminium oxide had a crystalline structure. The synthesised materials were also shown to offer excellent performance as catalysts of the conversion of ethanol at 600°C, the products being H_2 and CO (syngas).

Kraleva et al. [62] used the sol-gel method to obtain TiO_2/ZrO_2 systems with different contents of ZrO_2 (3, 6, 13 and 37% mol.). The synthesised materials were subjected to detailed physicochemical analysis. Analysis of their porous structure parameters showed that as the content of ZrO_2 increased, there was an increase in the BET specific surface area. X-ray spectroscopy revealed that the addition of zirconium dioxide also has a significant effect on the crystalline structure and the phase composition of the resulting oxide systems. The TiO_2/ZrO_2 system obtained with a ZrO_2 content of 37% mol., calcined at 550°C, exhibited an amorphous structure. It was also observed that as the calcination temperature increased, diffraction bands appeared corresponding to srilankite—a mineral containing oxygen, titanium and zirconium.

2.3. Hydrothermal route

The hydrothermal method is one of the most advanced techniques for obtaining metals and their oxides. Hydrothermal synthesis is a non-conventional method defined as crystal synthesis or crystal growth under high temperature and high pressure water conditions from substances which are insoluble at ordinary temperature and pressure (<100°C, <1 atm). Water may act both as a catalyst and as a component of the continuous phase during synthesis. Among the wet chemical preparation methods, the hydrothermal route has been recognised as an energy and time saver, with faster kinetics of crystallisation than classic co-precipitation or sol-gel methods. The hydrothermal method has proven to be an excellent method for the synthesis of powders, fibres, single crystals, monolithic ceramic bodies, and coatings on metals, polymers, and ceramics [63]. By adjusting simple parameters such as temperature, pressure or precursor concentration, it is possible to alter the characteristics of the product particles, e.g. crystalline phase and particle size. In the hydrothermal method, the temperature of crystallisation is usually lower than in a typical thermal process. The agglomeration of particles can be prevented by carrying out crystallisation under high pressure. The products obtained without calcination and grinding are of high quality. Using this method, it is

possible to control the shape and size of particles; nonetheless, the process is slow and is unsuitable for use on an industrial scale [64].

Chae et al. [65] report the synthesis of titanium dioxide using titanium tetraisopropoxide (TTIP) as the precursor of TiO_2 in an ethanol–water mixture as solvent. TTIP was added dropwise to a mixture of ethanol, water and nitric acid with pH = 0.7. After being well stirred, the solution underwent a reaction in a hydrothermal reactor at 240–300°C for 4 h. X-ray diffraction (XRD) analysis showed that hydrothermal processing at 240–260°C leads to a product with the greatest crystallinity, containing an anatase crystalline phase and a small quantity of brookite. Increasing the temperature of the hydrothermal reaction above 260°C caused the formation of agglomerates of primary particles. The size of the particles was strongly influenced by the concentration of the titanium dioxide precursor and by the molar ratio of ethanol to water and less so by the temperature and time of the reaction. An increase in the ethanol:water molar ratio led to smaller particles; also, when that ratio exceeded 8, a less crystalline product was obtained, with a tendency for the formation of aggregates. An increase in the concentration of TTIP in the reaction mixture retarded the increase in particle size. Porous structure analysis confirmed that smaller particle sizes in the resultant materials corresponded to higher specific surface areas.

Zhang et al. [66] used the hydrothermal method to obtain TiO_2 nanowires with anatase crystalline structure. An appropriate quantity of white TiO_2 powder with anatase structure was placed in a teflon-lined autoclave, and 10 M NaOH was added up to 80% of the capacity of the reactor. The mixture was heated for 24 h at 200°C, and the product was then dried for 6 h at 70°C. The resulting material underwent detailed analysis using X-ray diffraction (XRD) and scanning, transmission and high-resolution electron microscopy (SEM, TEM, HRTEM). XRD analysis confirmed the very high purity of the product. SEM images showed the titanium dioxide to have the form of numerous nanowires with uncontaminated surfaces. It was also found that the product had an anatase crystalline structure. The obtaining of titanium dioxide in nanowire form was conditional on the use of NaOH, which acted as a "soft" matrix and on the high process temperature. A lower reaction temperature would favour the formation of titanium nanorods. Advantages of the reported process include its low cost, the high purity of the products, and the large number of TiO_2 nanowires produced.

Caillot et al. [67] carried out hydrothermal synthesis of TiO_2/ZrO_2 oxide systems. It was determined how the process conditions affected the morphology, crystalline structure and specific surface area of the products. The precursors used were zirconium oxychloride ($ZrOCl_2 \cdot 8H_2O$) and titanium tetrachloride ($TiCl_4$), which were added to a solution of ammonia water ($NH_3 \cdot H_2O$). Hydrothermal processing took place at a temperature of 220°C under a pressure of 25 bar for 4 h. The resulting sample was dried at 120°C and finally calcined at 500°C for 10 h. Thermogravimetric analysis of the TiO_2/ZrO_2 system following the hydrothermal process showed it to have high thermal stability. The diffractogram obtained for TiO_2/ZrO_2 following calcination at 500°C indicated an amorphous structure. Porous structure analysis showed the oxide system to have a specific surface area of 209 m^2/g.

Hirano et al. [68] investigated the catalytic properties and thermal stability of materials consisting of titanium dioxide and zirconium dioxide, obtained by the hydrothermal route from

$TiOSO_4$ (titanium(IV) sulphate(VI)) and $ZrCl_4$ (zirconium tetrachloride). Solutions were placed in hydrothermal reactors and heated at a temperature of 200 or 240°C for 48 h. The precipitate was dried at 60°C. Samples were additionally heated for 1 h at temperatures ranging from 400 to 1000°C. Diffractograms obtained for samples following hydrothermal treatment at 240°C for 48 h indicate the increasing presence of the monolithic structure of ZrO_2 as the concentration of Zr in the initial solution increases. Diffraction bands corresponding to anatase are also visible. Transmission electron spectroscopy showed that the addition of ZrO_2 causes a decrease in the sizes of crystallites. The photocatalytic activity of the products was tested in the decomposition of methylene blue (MB) under ultraviolet radiation. The TiO_2/ZrO_2 systems exhibited higher photocatalytic activity than a material consisting of pure TiO_2.

2.4. Solvothermal method

The solvothermal method is similar to the hydrothermal method, the difference lying in the type of solvent used: in the hydrothermal method it is water, while in the solvothermal method, it is a non-aqueous solvent. The range of temperatures used in the solvothermal method can be much greater than in the hydrothermal method and depends on the boiling point of the organic solvent used. In the solvothermal method, the control of the shape, size and crystallinity of TiO_2 particles is easier than in the hydrothermal method. The solvothermal method is considered a universal method for obtaining nanoparticles with a narrow range of size distribution. Using the solvothermal method, TiO_2 nanoparticles or nanotubes can be produced with or without a surfactant [69, 70].

Zhu et al. [71] described a method for obtaining mesoporous TiO_2 microspheres by a solvothermal route. The precursor used was titanium tetrabutoxide (TBOT), which was added to a solution of polyetherimide (PEI) and anhydrous alcohol. The resulting white suspension was transferred to an autoclave, where a reaction was carried out at 180°C for 24 h. The white precipitate was then washed with water and ethanol, dried for 6 h at 60°C, and calcined for 2 h at 400 or 500°C. The product was analysed using the XRD, SEM, TEM, HRTEM, XPS and BET techniques and UV-Vis absorption spectra. Photocatalytic activity was investigated based on the reaction of degradation of phenol and methyl orange (MO) under sunlight. Mesoporous anatase TiO_2 microspheres with high crystallinity were successfully obtained by the solvothermal method and exhibited high photocatalytic activity for both phenol and methyl orange.

The solvothermal method was used by Yang et al. [72] to synthesise titanium dioxide from titanium(IV) fluoride, which was dissolved in a mixture of deionised water and hydrochloric acid (used to stabilise the pH). The mixture was added, together with propan-2-ol and hydrofluoric acid, to a teflon-lined stainless steel autoclave. The reactor was placed in an electric oven at 180°C for between 5.5 and 44 h. X-ray analysis of the product showed the synthesised TiO_2 to have an anatase structure. The average particle size in the system was measured by scanning electron microscopy at 1.09 μm. Porous structure analysis showed the specific surface area of the titanium dioxide to be 1.6 m^2/g.

Oshima et al. [73] used the solvothermal method to obtain TiO_2 nanoparticles. Here, a polymer gel was used, which enabled strongly dispersed and homogeneous particles to be obtained. First, polyvinyl alcohol (PVA) was dissolved in water at 70°C. The reaction mixture was then cooled

http://dx.doi.org/10.5772/intechopen.69357

to room temperature; next, the precursor of titanium dioxide [$(NH_4)_8(Ti_4(C_6H_4O7)_4(O_2)_4 \cdot 8H_2O$] was added, and water was evaporated off using microwaves. The resulting polymer gel was mixed with ethanol, which served as a solvent, and the mixture was placed in an autoclave and heated for 18 h at 230°C. Finally, the product was dispersed in water at 50–70°C. X-ray analysis showed that prior to the solvothermal process, the material had an amorphous structure, but the diffractograms obtained for the titanium dioxide following solvothermal treatment contained peaks indicating formation of the anatase crystalline structure. The particle size distribution was found by transmission electron microscopy to lie within the range 4.4–6.8 nm. Physicochemical analysis confirmed the soundness of the method used to obtain titanium dioxide, and that it leads to homogeneous particles without a tendency to form agglomerates.

Supphasrirongjaroen et al. [74] used the solvothermal method to synthesise TiO_2/SiO_2 and TiO_2/ZrO_2 systems. It was investigated how the addition of Si or Zr affected the photocatalytic activity of the oxide system. Titanium tetraisobutanol (TNB), tetraethoxysilane (TEOS) and zirconium tetraisobutanol were used as sources of titanium, silicon and zirconium. Titanium dioxide with admixed SiO_2 and ZrO_2 was obtained by dissolving TEOS and zirconium tetraisobutanol in toluene. The resulting materials were placed in an autoclave (300°C, 2 h). The synthesis products were subjected to physicochemical analysis to determine how the process temperature affects the photocatalytic activity of the product. It was found that the samples treated at room temperature have higher photocatalytic activity. The process temperature was also found to have a significant effect on the specific surface area: in almost every case, the surface area was larger for the samples that had undergone calcination at 350°C. It was also found that the materials containing zirconium exhibited higher photocatalytic activity than those with silicon. The researchers concluded that the addition of an appropriate metal can improve the physicochemical properties of inorganic materials.

A study of the literature shows that research on the synthesis of advanced materials based on titanium dioxide is chiefly focused on the skilful control of processes (through appropriate choices of methods and conditions) serving to generate changes in the properties of those materials. Key factors include the selection of appropriate raw materials, optimization of the pH of the reaction system, modification of the relative quantities of reagents and selection of an optimum temperature for thermal processing. These process parameters make it possible to synthesise materials with controlled physicochemical and structural properties, including grain size and shape, degree of crystallinity, crystallite size and phase or surface composition, as well as chemical and thermal stability. Temperature has a particularly significant effect on the crystalline structure of materials based on TiO_2, which in turn determines their potential applications. This applies both to the calcination temperature and to the conditions of synthesis. It is of particular interest to carry out reactions in hydrothermal or solvothermal conditions, leading to products not only having a precisely designed crystalline structure—with the use of a much lower temperature than in other conventional methods—but also exhibiting a unique and diverse morphology. These methods also enable greater control of the size and shape of particles. A fundamental weakness of these processes, however, is the difficulty of increasing their scale. When selecting an appropriate method for the synthesis of titanium dioxide or hybrid materials incorporating it, attention should be given to the possibility of obtaining those

products on semi-industrial or full industrial scale. The transfer of optimum conditions of synthesis from the laboratory to larger-scale processes is often problematic and should continue to be the subject of intensive research.

3. Titanium dioxide–based hybrid materials as active photocalatysts

Photocatalysis is a phenomenon in which chemical reactions are accelerated by the action of light. The most important stage of the process is the light-induced excitation of electrons from the valence band to the conduction band. This takes place provided that the energy of the incident radiation is equal to or greater than the band gap of the photocatalyst and leads to the creation of electrons (e^-) and holes (h^+). The electrons combine with atmospheric oxygen to produce active O_2, while the holes combine with water or atmospheric water vapour to form OH• radicals. These hydroxide radicals are strong oxidising agents and can thus easily oxidise and decompose various organic pollutants (such as oils and fats). The active oxygen, on the other hand, triggers reduction reactions. In the photocatalysis process, oxidation and reduction reactions occur simultaneously. During photocatalysis, the created electrons and holes are subject to surface or voluminous recombination as well as taking part in redox reactions. The process of photocatalysis is affected by a number of factors: rate of reaction, mass of catalyst, wavelength, initial reagent concentration and luminous flux [75–80].

A key factor in the process is the photocatalyst used. Many semiconductor materials are available on the market for use in photocatalysis processes, but efforts are constantly being made to develop new materials that are highly active in the visible and near ultraviolet ranges, while also being biologically inert and photostable [81]. Among the wide range of photocatalysts in use, the most promising material is TiO_2, in view of its high photochemical activity. It is also regarded as a cheap, nontoxic material that is photostable and chemically and biologically inert [82].

Research has been carried out to investigate photocatalytic activity using two forms of TiO_2: anatase and rutile. The amorphous form of TiO_2 is considered to exhibit practically no such activity [83]. Photocatalytic activity is affected not only by the type of photocatalyst used, but above all by its physicochemical properties: specific surface area and pore type, degree of hydroxylation of the surface, particle size and degree of agglomeration and the degree of crystallinity and number of defects in the crystalline structure [84]. Differences in the performances of photocatalysts are attributed largely to physicochemical properties such as the width of the band gap, the rate of recombination of e^-–h^+ pairs and the number of hydroxyl groups on the TiO_2 surface.

The phase composition of the studied material is a very important factor in determining the photocatalytic activity of TiO_2. It has been frequently reported that anatase exhibits much greater photoactivity than rutile [85–87]. Tanaka et al. [88] and Kumar et al. [89] have suggested that the higher activity of anatase results from its lower capacity to adsorb oxygen, the higher degree of hydroxylation of the TiO_2 surface and the high specific surface area, which provides more active sites for the adsorption of pollutants. Too high a surface area entails

the presence of a large number of structural defects, which means that the recombination of charge carrier pairs proceeds much more rapidly. The recombination rate is slowed by a larger number of OH^- groups on the photocatalyst surface, which trap the holes generated [83, 90–92].

Titanium dioxide is the most widely used catalyst for photocatalytic degradation of organic compounds, but there are some limitations in using TiO_2 for practical applications, which include:

- its large band gap;
- its low quantum yield;
- the low photon utilisation efficiency,
- the narrow available light spectrum (UV is the most responsive range).

Various strategies have been adopted for improving or enhancing the photocatalytic efficiency of TiO_2 (see **Figure 3**). These methods can be summarised as either morphological modifications, such as increasing surface area and porosity, or chemical modifications, by the incorporation of additional components into the TiO_2 structure. Modifications include:

- the addition of transition metal ions (such as Cr, V, Zr, Mn, Fe, Mo) [93–96];
- preparation of the reduced form TiO_{2-x};
- sensitisation using dyes [97–100];
- doping with non-metals (such as N, S, C) [78, 101–103];
- use of hybrid semiconductors such as TiO_2/SiO_2, TiO_2/Al_2O_3, etc. [10, 104, 105].

Table 3 contains information on selected methods of modifying titanium dioxide.

The absorption spectrum for titanium dioxide can be shifted towards the visible range by the incorporation of additional particles which cause significant changes in the material's semiconductor properties. Doping was the first technique used by researchers to modify the

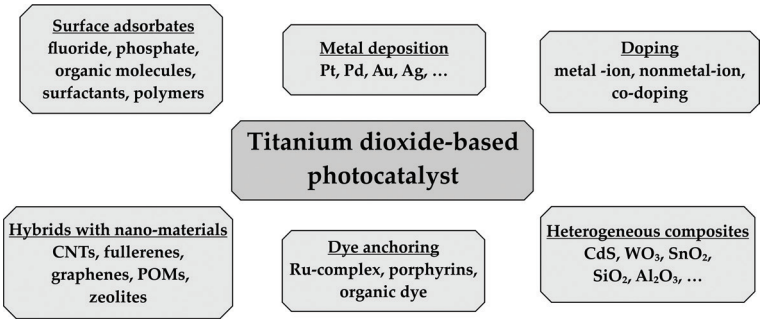

Figure 3. Various modification methods for titania-based photocatalysts.

Dopant	Precursor	Type of matrix	Conditions of preparation	Properties of obtained material	Potential application	Ref.
Doping with non-metal						
Iron	$FeCl_3 \cdot 6H_2O$, $TiCl_3$, $NH_3 \cdot H_2O$, HCl	–	Solution containing $TiCl_3$, ammonia and water was mixed at room temperature for 16 h, final pH = 8.5; hydrothermal treatment: 24 h at 110°C; drying: 80°C for ≥10 h, calcination: 500°C for 4 h	Anatase structure, the particle diameter decreases (from 25 to 15 nm) while the specific surface area increases (from 50 to 76 m^2/g) with the increasing iron content	Photodegradation of phenol	[106]
Tungsten	$Ti(OC_2H_5)_4$, toluene, $W(OC_2H_5)_5$	–	The resulting solution was stirred for 30 min and then atomised; the substrate temperature was kept at 500°C; deposition time was 45 min	Anatase structure	Destruction of resazurin redox dye	[107]
Doping with non-metal						
Nitrogen	NH_3 gas	TiO_2 nanorods prepared by hydrothermal route on a fluorine-doped tin oxide (FTO)-coated glass substrate	Thermal treatment of TiO_2 nanorods at 500°C for 1 h in the presence of NH_3 gas	Morphology: sample NTR-60—TiO_2 rods ~50 nm in length, sample NTR-150—TiO_2 rods ~900 nm in length and ~95 nm in width, rutile structure	Photooxidation of thiol molecules to the sulfonic acid species	[108]
	Trimethylamine	TiO_2 nanorods synthesised by the hydrothermal treatment	Hydrothermal treatment of TiO_2 at 200°C for 120 min with different amount (from 1 to 5% w/w compared to TiO_2) of trimethylamine	Anatase structure, crystallite size: is decreasing from 22 to 10 nm with increasing of N content, band gap: is decreasing from 3.22 to 2.85 eV with increasing of N content, BET surface area: from 81 to 101 m^2/g	Photodegradation of methyl orange (MO)—90% for sample NTO-4 (doping with 3%w/w N)	[109]

Dopant	Precursor	Type of matrix	Conditions of preparation	Properties of obtained material	Potential application	Ref.
Sulphur	Titanium butoxide, thiourea, methanol	–	Solution containing precursor of Ti with methanol was mixed with mixture of thiourea and methanol. Then obtained sample was calcined at 400, 500, 600 and 700°C for 3 h	Crystalline structure: sample calcined at 400–600°C—anatase structure, sample heated at 700°C—anatase and rutile structure, crystallite size: from 9 nm (sample TiS-400) to 50 nm (sample TiS-700), band gap: is decreasing from 3.21 to 3.07 eV with calcination treatment	Photodegradation of 4-chlorophenol—under UV light—98%—sample TiS-700, under visible light—40%—sample TiS-500	[110]
	Thiourea, ethanol, titanium tetraisopropoxide	–	Sample S-TiO_2: to solution containing thiourea and ethanol was added titanium tetraisopropoxide stirred at room temperature under aerated conditions for 48 h, calcination at 450°C for 4 h, sample S_8-TiO_2: pure, amorphous TiO_2 and S_8 were mixed and ground together thoroughly with a mortar, followed by annealing at 350°C for 4 h	Anatase structure, crystallite size: 13 nm for S-TiO_2 and S_8-TiO_2, and 14 nm, for TiO_2, particle size of 5–15 nm, BET surface area: 93 m^2/g for S-TiO_2 and 69 m^2/g for pure TiO_2		[111]
Heterogeneous composites						
ZnO	$Zn(NO_3)_2{\cdot}6H_2O$, hexamethylenetetramine (HMT, $C_6H_{12}N_4$)	The 3 durchin-like TiO_2 nanospheres	Hydrothermal synthesis: 100°C for 3 h, drying: 60°C	Anatase TiO_2 and hexagonal wurtzite-type ZnO, BET surface area—187 m^2/g	Photodegradation of nitrophenol and methyl orange	[112]
ZrO_2	Pluronic P123, $ZrOCl_2{\cdot}8H_2O$, titanium(IV) n-butoxide, HCl, C_2H_5OH	–	Synthesis: HCl + titanium(IV) n-butoxide + P123 in ethanol + $ZrOCl_2{\cdot}8H_2O$; deposition of thin film on indium tin oxide; calcination: 350, 400, 450, 500 and 800°C for 4 h	Anatase, rutile and tetragonal ZrO_2, BET surface area from 187 to 219 m^2/g,	Photodegradation of rhodamine B	[113]
	Ethanol, Pluronic P123, Macrogol 20000, titanium butyrate (TBT), HNO_3, $ZrOCl_2{\cdot}8H_2O$	–	Synthesis: ethanol, Pluronic P123, Macrogol 20000, titanium butyrate (TBT), HNO_3—room temparature, after adding $ZrOCl_2{\cdot}8H_2O$—80°C; calcination: 800°C for 5 h	Anatase structure, BET surface area—149 m^2/g	Photodegradation of rhodamine B	[59]

Dopant	Precursor	Type of matrix	Conditions of preparation	Properties of obtained material	Potential application	Ref.
Hybrids with nano-materials						
Graphene	Graphene oxide, poly(L-lysine) (PLL), ethylene glycol (EG)	TiO_2 hollow microspheres	Solvothermal method	–	Decomposition of MB dye	[114]
	Graphite powder, titanium dioxide, HCl, methanol, H_2SO_4, $KMnO_4$, H_2O_2, $NaNO_3$, methanol	–	Simple mixing at room temperature for 24 h and sonication, drying: dried in oven at 60°C	Anatase and rutile structure	Photodegradation of rhodamine B	[115]

Table 3. Modification of titanium dioxide.

electron structure of titanium dioxide [116]. Foreign ions or atoms are introduced into the titanium dioxide crystalline lattice with the aim of modifying and improving its physicochemical properties. The success of the process is largely dependent on the type and the quantity of dopant, which usually does not exceed a few percent. Both metals and non-metals may be used as dopants in titanium dioxide [83, 117–120].

The incorporation of metals (iron, chromium, tungsten, platinum, etc.) into titanium dioxide leads to a reduction in the band gap and thus an increase in absorption of radiation in the UV-Vis range. The activity of TiO_2 doped with metal ions depends largely on the valence of the dopant. If those ions have the same charge as the Ti ion in the crystal, the effect will be a change in the interactions between the metal atoms. The incorporation of metal ions of lower valence than Ti^{4+} (Y^{3+}, La^{3+}, Nd^{3+}, Pd^{2+}) favours a change in the size of the band gap and a reduction in the density of point defects [121–124].

Reports on the doping of titanium dioxide with iron confirm that the quantity of iron used, which may range from 0.05 to 50% Fe, has a significant effect on the increase in photocatalytic activity. In this process, a titanium atom in the anatase phase may be subject to substitution or else some of the iron atoms are incorporated into the titanium dioxide crystal lattice in anatase form to produce a composite, while some aggregates form the oxides Fe_2O_3 and Fe_3O_4. The doping process leads to the generation of shallow charge traps in the crystal structure, which decreases the recombination rate of electron-hole pairs. Introducing iron ions into the TiO_2 lattice not only leads to a lower electron-hole recombination rate but also increases excitability by visible light. Titanium dioxide doped with iron exhibits better photocatalytic activity under UV and also under visible light irradiation [106, 125–129].

The doping of TiO_2 with chromium not only increases its photocatalytic activity but also causes the photocatalyst to acquire ferromagnetic properties without losing its conductive properties. The enhancement of photocatalytic activity results from the formation of vast oxygen vacancies. The oxygen vacancies in TiO_2 act as electron traps which can bind the photoinduced electrons and play a significant role in inhibiting the recombination rate of photoinduced electron-hole pairs [130]. In turn, tungsten can be incorporated into the TiO_2 structure in oxide form (WO_x). This enhances the material's photocatalytic activity by reducing charge carrier recombination and by increasing light absorption in the visible portion of the spectrum [131].

Doping with non-metals is usually carried out to extend the photocatalytic activity of TiO_2 in the UV-Vis range. The introduction of non-metals into the oxygen sub-lattice may cause a change in the position of the valence band and thus reduce the band gap. Promising results have been obtained by doping titanium dioxide with non-metals such as nitrogen, carbon, iodine, sulphur and fluoride. Such doping narrows the band gap or leads to the appearance of new internal levels between the valence band and the conduction band [108–111]. When TiO_2 is doped with nitrogen, the dopant may replace an oxygen ion (in the case of a material with anatase structure) or a titanium ion (in the case of a rutile structure) [108, 109]. In case of doping with carbon, the dopant may replace oxygen or titanium or else occupy an inter-nodal position, depending on the energy of formation of the product and the presence of oxygen in the reaction environment. If doping is carried out in oxygen-rich conditions,

substitution of carbon for titanium takes place or else it is incorporated in the inter-nodal position due to its small atomic size. If the environment contains little oxygen, the carbon atom takes the oxygen position, forming the structure C-Ti-O-C [117, 132, 133]. The doping of titanium dioxide with iodine, on the other hand, leads to increased visible light absorption and increased photocatalytic activity below the visible range. This phenomenon results from retardation of the recombination of electron-hole pairs due to the capture of electrons by the iodine. Substitution of iodine atoms for oxygen or titanium results in a narrowing of the band gap [134]. Doping titanium dioxide with sulphur is more difficult, due to the fact that the dopant replaces oxygen in the oxide crystal lattice, and the differences in the radii of the two atoms are significant [110, 111].

Reports on the doping of titanium dioxide indicate that a small quantity of dopant will not lead to major changes in the porous structure but may cause significant changes in the phase composition of TiO_2 and in the size of crystallites. In the case of doping with nitrogen, an increase in the quantity of the dopant has been found to increase the thermal stability of anatase and to alter the temperature of transformation of anatase to rutile [135–137].

Another method for modifying the electron structure of titanium dioxide is the formation of hybrid oxide systems. Among synthetic hybrid oxide systems, TiO_2/ZrO_2 materials, which thanks to the addition of zirconium dioxide have much greater surface area and mechanical strength than pure TiO_2, deserve special attention. An admixture of ZrO_2 prevents the phase change of anatase to rutile and causes a reduction in the particle diameter of the resulting hybrid. These factors contribute to the improved photocatalytic activity of TiO_2/ZrO_2 oxide systems. There are many publications with information on the application of TiO_2/ZrO_2 hybrids in photocatalysis. The use of TiO_2/ZrO_2 hybrid materials in the photo-oxidation of organic compounds or degradation of dyes originating from various industrial processes is well known. It also has applications in the photo-reduction of atmospherically harmful oxides, like CO_2 and NO_x, resulting for example from the combustion of fossil fuels. The advantages of the TiO_2/ZrO_2 hybrid are its mechanical strength, nontoxicity and corrosion resistance and the ability to conduct photocatalytic processes using sunlight. These advantages may stimulate increasing demand for this material in the near future [59, 113, 138].

Zhou et al. [113] determined the photocatalytic properties of a TiO_2/ZrO_2 system obtained by the sol-gel method. Physicochemical analysis showed the products to have an anatase crystalline structure. An increase in the molar content of zirconium dioxide leads to a decrease in the crystallinity of the resulting materials, while an increase in the temperature of calcination increases their crystallinity. The specific surface areas of the materials (for all variant methods of synthesis) lay in the range 187.0–219.2 m^2/g. Photocatalytic analysis indicated a fall in the effectiveness of photocatalysis as the temperature of calcination of the materials was increased.

The sol-gel method was also used by Fan et al. [59] to obtain a TiO_2/ZrO_2 system. It was found that the proposed method led to mesoporous materials with a well-crystallised anatase structure. The systems were found to have high specific surface areas, in the range 136.9–148.9 m^2/g.

Combining titania with zinc oxide can also lead to a hybrid oxide system with good photocatalytic properties. The resulting material can be used, for instance, in the degradation

of organic impurities such as detergents, dyes and pesticides present in various types of wastewater. The TiO_2/ZnO hybrid material can be synthesised by both physical and chemical processes, which enables enhancement of its properties, for example by widening its light absorption spectrum. Additionally, the photocatalytic activity of oxides may help reduce the susceptibility of pollutants to form aggregate structures [139].

Cheng et al. [140] determined the photocatalytic properties of a hybrid material (UTZ) consisting of 3D nanospherical TiO_2 with a "hedgehog" shape and one-dimensional ZnO in the form of "nanospindles". The resulting system was highly homogeneous and contained the crystalline structure of anatase (TiO_2) and the hexagonal wurtzite structure (ZnO). The TiO_2/ZnO system was found to offer significantly better photocatalytic performance than pure ZnO or TiO_2 in the decomposition of methyl orange (MO) and nitrophenol. This high photocatalytic activity was probably due to the existence of a closely bound heterostructural surface between the ZnO and TiO_2, enabling charge separation and reducing the rate of recombination of electron-hole pairs.

The marked improvement in photocatalytic activity in the case of titania/graphene hybrids is linked to the fact that the graphene component enables the transfer and/or trapping of electrons photogenerated in the oxide semiconductor structure, allowing the holes to form reactive sites. Therefore, charge recombination is suppressed, leading to improvement of the photocatalytic performance [141].

Yan et al. [114] obtained a novel three-dimensional (3D) reduced graphene oxide/TiO_2 (rGO/TiO_2) hybrid composite by wrapping TiO_2 hollow microspheres with rGO sheets via a facile solvothermal route using poly(L-lysine) (PLL) and ethylene glycol (EG) as coupling agents. It was confirmed that the hybrid materials, containing mixed phases of TiO_2 (with content of rutile - 20.8%), demonstrate higher photocatalytic activity in the decomposition of MB dye. Ni et al. [142] synthesised high-photoactive GP strongly wrapped three-dimensional anatase TiO_2. The prepared material demonstrated excellent photocatalytic activity under UV irradiation for the degradation of MB, much higher than that of commercial P25 titania. Similar results were presented by Thomas et al. [115], who synthesised high-performance functionalised FLG (FFLG) decorated with TiO_2 photocatalyst, by simple mixing without any calcination or high-pressure treatment. The FFLG/TiO_2 system produced a higher rate of degradation of Rhodamine B (Rhd B) as compared with pure TiO_2 nanoparticles and FLG-TiO_2 (non-functionalised FLG).

Although titanium dioxide is an excellent candidate for photocatalytic applications, due to its band gap size, nontoxicity, chemical stability, inert nature and relatively low cost, it is subject to certain limitations, chiefly resulting from its relatively low activity in the visible light range and its high exciton recombination rate. For this reason, much research is carried out with the aim of improving and reinforcing the photocatalytic activity of TiO_2 and increasing its spectral sensitivity. This may be achieved by modifying TiO_2 during or after its synthesis, with the choice of a suitable method of activation (doping with metals or nonmetals, coupling with other semiconductor materials, increasing its crystallinity by calcination, or synthesis of hybrid materials). These solutions can lead to a material with enhanced photocatalytic properties, including increased sensitivity in the UV and visible light ranges, and with reduced recombination rate due to the provision of charge traps. New research trends also relate to

the combination of TiO_2 with polymers or various forms of carbon nanotubes, fullerenes, graphene oxide (GO) or reduced GO (R-GO), with the aim of obtaining multifunctional materials with a wide range of applications. With this in mind, it should be emphasised how many opportunities and technological solutions are available for implementation with the goal of obtaining unique titania-based materials.

4. Titanium dioxide derivatives as effective electrode materials

Recent years have seen intense development in research aimed at seeking new materials and design solutions to enable further progress in the technology of lithium-ion batteries, which are seen as one of the leading technologies for energy storage. Currently, the greatest challenge in the design of these batteries is to find an optimum combination of cathode and anode materials, as these largely determine the cell's parameters, including capacity, voltage, reversibility of the charge/discharge reaction, and chemical stability. The electrode materials must not only be compatible with each other but also should form a synergic system together with the electrolyte and separator [143–145].

Among a range of available materials, titanium dioxide and its derivatives have recently gained popularity as anodes for Li-ion batteries because they allow the design of operational devices with only minor safety concerns. This class of materials offers improved chemical and thermal stability, low cost, biocompatibility, relatively high surface area and porosity, a broad electrochemical window, rate capability and enhanced cyclic performance by virtue of their superior electrical conductivity. These features make titania-based derivatives a good candidate to replace the commonly used carbon (graphene) as an anode material in LIBs. However, limitations include the low capacity, low electrical conductivity, poor rate capability and poor cycling performance of titanium dioxide. Much research has been carried out to overcome the difficulties related to the use of TiO_2 as an electrode material. Numerous scientific centres worldwide are working on ways of improving the electrochemical behaviour of titania and its derivatives. The chief aim is to enhance the electronic conductivity by producing different titania nanostructures to increase its capacity through the incorporation of selected metal oxides into its structure. Another approach is to combine or coat TiO_2 with carbonaceous materials or to introduce anionic or cationic dopants to form more open channels and active sites for Li ion transport [143–149].

Moreover, the electrochemical performance and the lithium intercalation/de-intercalation processes of titania-based materials typically depend on their crystallinity, structure, morphology, particle size and surface area. In particular, it has been found that nanostructured titanium oxide leads to better capacity, longer cycling life and higher rate capability than the bulk materials. Titania has several allotropic forms, the best-known being tetragonal rutile and anatase, and orthorhombic brookite. Even though anatase has been considered the most electroactive form, other allotropes such as rutile and brookites are also widely studied for potential use as anodes. Moreover, synthesis of this type of system can effectively improve their capacitive performance by creating products with excellent high-rate cycling ability and stability. The application of such hybrid materials as anodes in lithium-ion batteries should

lead to charge redistribution in the lattice, facilitate the diffusion of Li^+, and finally increase lattice defects and conductivity [145–152].

Kubiak et al. [153] investigated the electrochemical performance of a mesoporous TiO_2 synthesised via a sol-gel method utilising an ethylene glycol-based titanium precursor in the presence of an amphiphilic molecule as the templating agent. The obtained material presents pure anatase TiO_2 without the presence of other phases, with a monomodal pore diameter close to 5 nm and BET surface area of 92 m^2/g. The mesoporous anatase titania shows excellent rate capability (184 mAh/g at C/5, 158 mAh/g at 2C, 127 mAh/g at 6C, and 95 mAh/g at 30C) and good cycling stability. The authors concluded that the electrochemical performance of anatase titania was determined not only by surface area and crystallite size but also by mesopore size. The presence of mesopores was important for high-rate performance and favourable to electrolyte ion transport.

Mancini et al. [154] found that new Cu or Sn/mesoporous anatase electrodes offer excellent electrochemical performance, especially in terms of fast insertion/extraction capacity. The capacity after 200 cycles is 123, 147 and 142 mAh/g for uncoated, Cu-coated and Sn-coated anatase electrodes, respectively, with capacity retention of about 80% for all electrodes. The good electrochemical behaviour of metal/mesoporous anatase TiO_2 is ascribed to the combined effects of mesopores and the electronically conductive metal layer. Moreover, the metal coating provides a lower polarisation of the electrodes, which indicates faster kinetics of the electrochemical processes. The researchers suggested that a thin metal coating may be a very promising method in the development of high-rate electrode materials for Li-ion batteries.

Kubiak et al. [155] produced nanosized rutile TiO_2 via a hydrolytic sol-gel route, applying a glycerol-modified precursor in the presence of an anionic surfactant. The proposed methodology led to rutile whiskers, which agglomerated to cauliflower-like aggregates of several micrometers, with a BET surface area of 181 m^2/g. This interesting morphology of rutile titania favours contact between the active material and the electrolyte. The obtained material shows excellent electrochemical performance in terms of capacity, cyclability, stability and reversibility, especially at high charge/discharge rates. The authors demonstrated that this high rate capability can be ascribed to shorter transport lengths for both electronic and Li^+ transport, as well as a larger electrode/electrolyte contact area due to the high surface area.

Mesoporous anatase TiO_2 was synthesised via a urea-assisted hydrothermal method by Jung et al. [156]. The authors investigated the influence of thermal treatment of mesoporous TiO_2 at 300, 400 and 500°C on its electrochemical performance. The prepared material was found to consist of monophasic TiO_2 sub-microspheres with uniform particle size (ca. 400 nm), a crystallite size of 14 nm and a BET surface area of 116 m^2/g. The capacity for the mesoporous TiO_2 calcined at 400°C after 80 cycles is 154 mAh/g, with capacity retention of about 94.5%. It was concluded that the large surface area introduced by the highly porous nano-structured building blocks of each TiO_2 sub-microsphere assisted in creating an easy and shorter diffusion pathway for ionic and electronic diffusion. These results indicate the good power performance of the synthesised material.

Zhang et al. [157] showed that hierarchical nanostructures and composition play key roles in the electrochemical performance of TiO_2 hollow microspheres used as anode materials. Mesoporous hollow TiO_2 microspheres with controlled size and hierarchical nanostructures were synthesised by hydrothermal methods. The results show that the hollow microspheres composed of mesoporous nanospheres exhibit a very stable reversible capacity of 184 mAh/g at 0.25C and an extremely high power of 122 mAh/g at the high rate of 10C. It was also shown that the hollow structure and large mesoporous channels of the material facilitate electrolyte transportation and lithium ion diffusion, and the small mesopores and small-sized nanoparticles increase the lithium storage capacity.

Metal oxides are one of the promising classes of materials to replace graphite anodes for LIBs, because these materials have diverse chemical and physical properties and can deliver high reversible capacities between 500 and 1000 mAh/g. The electrodes of metal oxides, which have high specific capacity, are prone to fail during their reaction with Li ions during the charge and discharge processes. To prevent these failures, TiO_2 is introduced into these electrodes to form TiO_2/metal-oxide composites. The TiO_2/metal-oxide composites for LIBs most commonly combine TiO_2, which has good cycling performance and capacity for LIBs, with other metal oxides with high capacity for LIBs such as SiO_2, ZnO, ZrO_2, etc [154, 155, 158].

Opra et al. [159] obtained nanostructured Zr-doped (1 at.%) TiO_2 (anatase) via a template sol-gel method on carbon fibre. The obtained material consisted of microtubes (length 10–300 μm, outer diameter 3–5 μm) composed of nanoparticles with a size of 15–25 nm. Moreover, Zr-doped TiO_2 shows significantly higher reversible capacity (140 mAh/g) after 20-fold cycling at a rate of 0.1C in the range 3–1 V in comparison with undoped titania (65 mAh/g). It was reported that the transport of Li^+ ions depends significantly on the structural characteristics of titania [17]. When Zr^{4+} ions are incorporated into the anatase structure, the difference in the ionic radii of the metal ions increases the lattice parameters and creates defects. The creation of defects leads to charge redistribution in the titania lattice and increases the conductivity (according to EIS results).

Gao et al. [160] reported the successful production of TiO_2/ZnO nanocomposite arrays for lithium-ion battery application. The sandwich-like TiO_2/ZnO framework with 3D interconnected construction shows stable cycling performance with a specific capacity of 340 mAh/g at a current density of 200 mA/g after 100 cycles. The authors noted that the uniform decoration of ZnO nanoparticles onto the TiO_2 nanosheet arrays plays a significant role in advancing their electrochemical performance.

Siwińska-Stefańska and Kurc [161] used a novel TiO_2-SiO_2-ZrO_2 (TSZ) ternary oxide system (with a TiO_2:SiO_2:ZrO_2 molar ratio of 8:1:1) synthesised via a sol-gel route as an anode material in a Li-ion battery. They combined titania with silica, which can react with a low discharge potential and can store a large quantity of lithium ions, as well as with zirconia, which is capable of suppressing SEI formation and enhancing electron transport to improve electrochemical performance. The specific discharge/charge capacity of the TSZ electrode is about 175 mAh/g.

Unique TiO_2 nanotube arrays (TNAs) grafted with MnO_2 nanosheets were synthesised as a Li-ion battery anode by Zhu et al. [162]. The obtained composite combines the advantages of both MnO_2, with its high capacity (1230 mAh/g), and TNAs, with excellent cycle stability

and superior electrical conductivity. Sample TM-10 demonstrated a capacity of 610 mAh/g at a current rate of 350 mA/g and a capacity of 385 mAh/g at a rate of 700 mA/g even after 700 cycles. It was proved that the layer thickness of MnO_2 has a major impact on electrochemical performance.

Research on anode materials for lithium-ion batteries has also been focused on carbonaceous materials and transmission semiconductors such as TiO_2. Carbonaceous materials have high stability, but low volumetric capacity, mainly due to their large initial irreversible capacity. Metal oxide semiconductors have many advantages as electrode materials, including robustness, chemical and thermal stability, low cost, biocompatibility, and relatively high electronic conductivity. The synthesis of mesoporous oxide semiconductors like titania has become an important issue in the construction of smart nanosensors with electrodes decorated by metal oxides [163–166].

Qiu et al. [167] synthesised a mesoporous TiO_2/graphene composite using graphene oxide (GO) and cheap $TiOSO_4$ as precursors, via a facile one-step hydrothermal route. The obtained material exhibited a high discharge capacity (141.7 mAh/g) at the current density 5000 mA/g, an impressive value which is among the highest measured for any TiO_2/graphene composite. The authors suggested that the conductive graphene in the composite may facilitate electron transfer and contribute to the higher rate capability of the TiO_2/graphene composite electrode compared with the blank TiO_2 electrode.

Carbon-coated TiO_2/SiO_2 nanocomposites (CTSO) were produced using a simple hydrothermal approach by Zhang et al. [168] as anode materials for lithium-ion batteries. The CTSO anode exhibits superior high-rate capability and excellent cycling performance. The specific capacity of the obtained material is much higher than that of pure TiO_2 and silica-modified TiO_2 without carbon nanocoating (TSO), which indicates that the material and structural hybridisation has a positive synergistic effect on the electrochemical properties. CTSO (0.05) presented the best cyclability, with 264 mAh/g retained after 270 cycles at 30 mA/g, and superior high-rate performance (233 mAh/g at 150 mA/g after 600 cycles, and even 167 mAh/g at 300 mA/g after 1000 cycles).

Siwińska-Stefańska and Kurc [169] reported on the synthesis, electrochemical properties and performance of a new type of microsized titania/graphene oxide (TA/GO) composite applied as a new anode material in lithium-ion batteries. The material was characterised by the presence of microsized particles with anatase and rutile structure, and a BET surface area of 6.2 m^2/g. The specific discharge and charge capacities of TA/GO electrodes are approximately 1850–2010 and 2050–2100 mAh/g, respectively. Strong Ti–O–C chemical bonds give the composite resilient strength to facilitate the ordered assembly of TiO_2 nanoparticles and formation of a mesoporous structure with a high tap density, enable the rapid transport of Li ions and electrons within the composite structure and maintain a stable mesoporous structure during the discharge/charge process of the resultant LIBs.

Mesoporous TiO_2/CNTs 3D conductive network hybrid nanostructures were synthesised using a facile PEO-aided self-assembled process by Wang et al. [170]. The material demonstrated high Li storage capacity, superior rate performance and excellent long-term cycling stability. Mesoporous TiO_2/CNTs exhibits a reversible specific capacity of 203 mAh/g at 100 mA/g and

a stable capacity retention of 91 mAh/g at 8000 mA/g (47.6C) over 100 cycles. The obtained material also retained approximately 90% (71 mAh/g) of its initial discharge capacity after 900 cycles at an extremely high rate of 15,000 mA/g (89C).

As this review of the subject literature shows, the search for new electrode materials is the subject of ongoing worldwide research efforts. The work is largely oriented towards the development of new types of batteries with high energy density and cyclability, and with as fast a charging rate as possible. The search for new electrode materials, and modification of existing ones, to achieve increased electrical capacity and the possibility of operation over a wider range of potentials relative to the lithium electrode is part of a current trend in scientific research.

Based on the current state of knowledge and our own research, we foresee continued growth in research work oriented towards the synthesis of functional materials containing titanium dioxide. Studies to date show that the obtaining of such materials is particularly important from both a theoretical and a practical standpoint. The good availability of methods for obtaining titania-based systems, their interesting physicochemical properties and their broad range of possible applications mean that these materials are coming to be used more and more widely in various branches of industry. Also of key importance is the synthesis of hybrid materials aimed at improving the physicochemical properties of TiO_2, including through the careful control of the quantities of particular components. This creates a wide area for potential research and represents an alternative to the popularly used methods of synthesis. Research in this area is directed towards obtaining functional materials with not only photocatalytic but also antibacterial properties, offering defined electrochemical or barrier effects. Also being intensively developed are combined methods, such as the microwave-assisted sol-gel process, which also introduce interesting theoretical considerations regarding the synthesis of titania-based materials. This creates better possibilities for control of the synthesis and of the physicochemical parameters of the products.

Analysis of the literature review presented confirms the justification for the continuation of research into the synthesis of functional materials based on TiO_2.

Acknowledgements

This work was supported by Poznan University of Technology research grant no. 03/32/DSPB/0706/2017.

Author details

Katarzyna Siwińska-Stefańska* and Teofil Jesionowski

*Address all correspondence to: katarzyna.siwinska-stefanska@put.poznan.pl

Faculty of Chemical Technology, Institute of Chemical Technology and Engineering, Poznan University of Technology, Poznan, Poland

References

[1] Wypych G. Handbook of Fillers. 2nd ed. Toronto: ChemTec Publishing; 1999. 912 p.

[2] Braun JH. Titanium dioxide: A review. Journal of Coating Technology. 1997;**69**(868):59-72

[3] Siwińska-Stefańska K, Krysztafkiewicz A, Ciesielczyk F, Paukszta D, Sójka-Ledakowicz J, Jesionowski T. Physicochemical and structural properties of TiO_2 precipitated in an emulsion system. Physicochemical Problems of Mineral Processing. 2010;**44**:231-244

[4] Winkler J. Titanium dioxide. Production, properties and effective usage. 2nd ed. Hanover: Vincentz Network; 2013. 150 p

[5] Chen X, Mao SS. Titanium dioxide nanomaterials: Synthesis, properties, modifications, and applications. Chemical Reviews. 2007;**107**(7):2891-2959. DOI: 10.1021/cr0500535

[6] Ragupathy S, Raghu K, Prabu P. Synthesis and characterization of TiO_2 loaded cashew nut shell activated carbon and photocatalytic activity on BG and MB dyes under sunlight radiation. Spectrochimica Acta Part A. 2015;**138**(5):314-320. DOI: 10.1016/j.saa.2014.11.087

[7] Azambre B, Zenboury L, Weber JV, Burg P. Surface characterization of acidic ceria-zirconia prepared by direct sulfation. Applied Surface Science. 2010;**256**(14):4570-4581. DOI: 10.1016/j.apsusc.2010.02.049

[8] Miller JM, Lakshmi LJ. Spectroscopic characterization of sol-gel-derived mixed oxides. The Journal of Physical Chemistry B. 1998;**102**(34):6465-6470. DOI: 10.1021/jp9810771

[9] Mohamed MM, Salama TM, Yamaguchi T. Synthesis, characterization and catalytic properties of titania-silica catalysts. Colloids and Surfaces A. 2002;**207**(1-3):25-32. DOI: 10.1016/S0927-7757(02)00002-X

[10] Tobaldi DM, Tucci A, Ŝkapin AS, Esposito L. Effects of SiO_2 addition on TiO_2 crystal structure and photocatalytic activity. Journal of the European Ceramic Society. 2010;**30**(12):2481-2490. DOI: 10.1016/j.jeurceramsoc.2010.05.014

[11] Wu ZY, Tao YF, Lin Z, Liu L, Fan XX, Wang Y. Hydrothermal synthesis and morphological evolution of mesoporous titania-silica. Journal of Physical Chemistry C. 2009;**113**(47):20335-20348. DOI: 10.1021/jp9037842

[12] Messina PV, Morini MA, Sierra MB, Schulz PB. Mesoporous silica-titania composed materials. Journal of Colloid and Interface Science. 2006;**300**(1):270-278. DOI: 10.1016/j.jcis.2006.03.039

[13] Nilchi A, Janitabar-Darzi S, Mahjoub AR, Rasouli-Garmarodi S. New TiO_2/SiO_2 nanocomposites—Phase transformations and photocatalytic studies. Colloids and Surfaces A. 2010;**361**(1-3):25-30. DOI: 10.1016/j.colsurfa.2010.03.006

[14] Hadjiivanov KI, Klissurski DG. Surface chemistry of titania (anatase) and titania-supported catalysts. Chemical Society Reviews. 1996;**25**(1):61-69. DOI: 10.1039/CS9962500061

[15] Scolan A, Sanchez C. Synthesis and characterization of surface-protected nanocrystalline titania particles. Chemistry of Materials. 1998;**10**(10):3217-3223. DOI: 10.1021/cm980322q

[16] Lal M, Chhabra V, Ayyub P, Maitra A. Preparation and characterization of ultrafine TiO_2 particles in reverse micelles by hydrolysis of titanium di-ethylhexyl sulfosuccinate. Journal of Materials Research. 1998;**13**(5):1249-1254. DOI: 10.1557/JMR.1998.0178

[17] Su C, Hong B-Y, Tseng C-M. Sol-gel preparation and photocatalysis of titanium dioxide. Catalysis Today. 2004;**96**(3):119-126. DOI: 10.1016/j.cattod.2004.06.132

[18] Yang P, Lu C, Hua N, Du Y. Titanium dioxide nanoparticles co-doped with Fe^{3+} and Eu^{3+} ions for photocatalysis. Materials Letters. 2002;**57**(4):794-801. DOI: 10.1016/S0167-577X(02)00875-3

[19] Bessekhouad Y, Robert D, Weber JV. Synthesis of photocatalytic TiO_2 nanoparticles: Optimization of the preparation conditions. Journal of Photochemistry and Photobiology A. 2003;**157**(1):47-53. DOI: 10.1016/S1010-6030(03)00077-7

[20] Kormann C, Bahnemann DW, Hoffmann R. Preparation and characterization of quantum-size titanium dioxide. Journal of Physical Chemistry. 1988;**92**(18):5196-5201. DOI: 10.1021/j100329a027

[21] Li B, Wang X, Yan M, Li L. Preparation and characterization of nano-TiO_2 powder. Materials Chemistry and Physics. 2002;**78**(1):184-188. DOI: 10.1016/S0254-0584(02)00226-2

[22] Kim C-S, Moon BK, Park J-H, Chung ST, Son S-M. Synthesis of nanocrystalline TiO_2 in toluene by a solvothermal route. Journal of Crystal Growth. 2003;**254**(3-4):405-410. DOI: 10.1016/S0022-0248(03)01185-0

[23] Wang C, Deng Z-X, Zhang G, Fan S, Li Y. Synthesis of nanocrystalline TiO_2 in alcohols. Powder Technology. 2002;**125**(1):39-44. DOI: 10.1016/S0032-5910(01)00523-X

[24] Kang M, Kim B-J, Cho SM, Chung C-H, Kim B-W, Han GY, Yoon KJ. Decomposition of toluene using an atmospheric pressure plasma/TiO_2 catalytic system. Journal of Molecular Catalysis A. 2002;**180**(1-2):125-132. DOI: 10.1016/S1381-1169(01)00417-4

[25] Kominami H, Kohno M, Takada Y, Inoue M, Inui T, Kera Y. Hydrolysis of titanium alkoxide in organic solvent at high temperatures: A new synthetic method for nanosized, thermally stable titanium(IV) oxide. Industrial & Engineering Chemistry Research. 1999;**38**(10):3925-3931. DOI: 10.1021/ie9901170

[26] Kolen'ko YV, Burukhin AA, Churagulov BR, Oleynikov NN. Synthesis of nanocrystalline TiO_2 powders from aqueous $TiOSO_4$ solutions under hydrothermal conditions. Materials Letters. 2003;**57**(5-6):1124-1129. DOI: 10.1016/S0167-577X(02)00943-6

[27] Zhang TC, Surampalli RY, Lai KCK, Hu Z, Tyagi RD, Lo IMC. Nanotechnologies for Mater Environment Application. Virginia: American Society of Civil Engineers; 2009. 630 p. DOI: 10.1061/9780784410301

[28] Michael D, Mingos P. Comprehensive Organometallic Chemistry III. 1st ed. Oxford: Elsevier Science; 2007. 958 p.

[29] Liu Z, Wang R, Kan F, Jiang F. Synthesis and characterization of TiO_2 nanoparticles. Asian Journal of Chemistry. 2014;**26**(3):655-659. DOI: 10.14233/ajchem.2014.15462

[30] Muhamed Shajudheen VP, Viswanathan K, Anitha Rani K, Uma Maheswari A, Savavana Kumar S. A simple chemical precipitation method of titanium dioxide nanoparticles using polyvinyl pyrrolidone as a capping agent and their characterization. International Journal of Chemical Molecular Nuclear, Materials and Metallurgical Engneering. 2006;**10**(5):552-555

[31] Huang M, Yu S, Lin B, Dongn L, Zhang F, Fan M, Wang L, Yu J, Deng Ch. Influence of preparation methods on the structure and catalytic performance of SnO_2-doped TiO_2 photocatalysts. Ceramics International. 2014;**40**(8):13305-13312. DOI: 10.1016/j.ceramint.2014.05.043

[32] Yu M, Li C, Zeng G, Zhou Y, Zhang X, Xie Y. The selective catalytic reduction of NO with NH_3 over a novel Ce-Sn-Ti mixed oxides catalyst: Promotional effect of SnO_2. Applied Surface Science. 2015;**342**:174-182. DOI: 10.1016/j.apsusc.2015.03.052

[33] Zhang Y, Zhu X, Shen K, Xu H, Sun K, Zhou Ch. Influence of ceria modification on the properties of TiO_2-ZrO_2 supported V_2O_5 catalysts for selective catalytic reduction of NO by NH_3. Journal of Colloid and Interface Science. 2012;**376**(1):233-238. DOI: 10.1016/j.jcis.2012.03.001

[34] Pierre AC, Pajonk GM. Chemistry of aerogels and their applications. Chemical Reviews. 2002;**102**(11):4243-4266. DOI: 10.1021/cr0101306

[35] Lu ZL, Lindner E, Mayer HA. Applications of sol-gel processed interphase catalysts. Chemical Reviews. 2002;**102**(10):3543-3578. DOI: 10.1021/cr010358t

[36] Wight AP, Davis ME. Design and preparation of organic-inorganic hybrid catalysts. Chemical Reviews. 2002;**102**(10):3589-3614. DOI: 10.1021/cr010334m

[37] Schwarz JA, Contescu C, Contescu A. Methods for preparation of catalytic materials. Chemical Reviews. 1995;**95**(3):477-510. DOI: 10.1021/cr00035a002

[38] Hench LL, West JK. The sol-gel process. Chemical Reviews. 1990;**90**(1):33-72. DOI: 10.1021/cr00099a003

[39] Arnal P, Corriu RJP, Leclercq D, Mutin PH, Vioux A. A solution chemistry study of nonhydrolytic sol-gel routes to titania. Chemistry of Materials. 1997;**9**(3):694-698. DOI: 10.1021/cm960337t

[40] Milea CA, Bogatu C, Duţă A. The influence of parameters in silica sol-gel process. Bulletin of the Transilvania University of Braşov Series I: Engineering Sciences. 2011;**4**(53):59-66

[41] Chan Y-L, Pung S-Y, Sreekantan S. Degradation of organic dye using ZnO nanorods based continuous flow water purifier. Journal of Sol-Gel Science and Technology. 2013;**66**(3):399-405. DOI: 10.1007/s10971-013-3022-9

[42] Wu L-A, Jiang X, Wu S, Yao R, Qiao X, Fan X. Synthesis of monolithic zirconia with macroporous bicontinuous structure via epoxide-driven sol-gel process accompanied

by phase separation. Journal of Sol-Gel Science and Technology. 2014;**69**(1):1-8. DOI: 10.1007/s10971-013-3157-8

[43] Ciesielczyk F, Przybysz M, Zdarta J, Piasecki A, Paukszta D, Jesionowski T. The sol-gel approach as a method of synthesis of $xMgO{\cdot}ySiO_2$ powder with defined physicochemical properties including crystalline structure. Journal of Sol-Gel Science and Technology. 2014;**71**(3):501-513. DOI: 10.1007/s10971-014-3398-1

[44] Vrancken KC, Possemiers K, Voort PVD, Vansant EF. Surface modification of silica gels with aminoorganosilanes. Colloids and Surfaces A. 1995;**98**(3):235-241. DOI: 10.1016/0927-7757(95)03119-X

[45] Cerveau G, Corriu RJP, Lepeytre C, Mutin PH. Influence of the nature of the organic precursor on the textural and chemical properties of silsesquioxane materials. Journal of Materials Chemistry. 1998;**8**(12):2707-2714. DOI: 10.1039/A805794J

[46] Corriu R. A new trend in metal-alkoxide chemistry: The elaboration of monophasic organic-inorganic hybrid materials. Polyhedron. 1998;**17**(5-6):925-934. DOI: 10.1016/S0277-5387(97)00261-1

[47] Corriu RJP, Leclerq D. Recent developments of molecular chemistry for sol-gel processes. Angewandte Chemie. 1996;**35**(13-14):1420-1436

[48] Shea KJ, Loy DA, Webster O. Arylsilsesquioxane gels and related materials. New hybrids of organic and inorganic networks. Journal of the American Chemical Society. 1992;**114**(17):6700-6710. DOI: 10.1021/ja00043a014

[49] Jackson CL, Bauer BJ, Nakatami AI, Barnes J. Synthesis of hybrid organic-inorganic materials from interpenetrating polymer network chemistry. Chemistry of Materials. 1996;**8**(3):727-733. DOI: 10.1021/cm950417h

[50] Attar AS, Ghamsari MS, Hajiesmaeilbaigi F, Mirdamadi S. Modifier ligands effects on the synthesized TiO_2 nanocrystals. Journal of Materials Science. 2008;**43**(5):1723-1729. DOI: 10.1007/s10853-007-2244-z

[51] You JH, Hsu KY. Influence of chelating agent and reaction time on the swelling process for preparation of porous TiO_2 particles. Journal of the European Ceramic Society. 2010;**30**(6):1307-1315. DOI: 10.1016/j.jeurceramsoc.2009.10.011

[52] Huang T, Huang W, Zhou C, Situ Y, Huang H. Superhydrophilicity of TiO_2/SiO_2 thin films: Synergistic effect of SiO_2 and chase-separation-induced porous structure. Surface & Coatings Technology. 2012;**213**:126-132

[53] Chang JA, Vithal M, Baek IC, Seok SI. Morphological and phase evolution of TiO_2 nanocrystals prepared from peroxotitanate complex aqueous solution: Influence of acetic acid. Journal of Solid State Chemistry. 2009;**182**(4):749-756. DOI: 10.1016/j.jssc.2008.12.024

[54] Faycal Atitar M, Ismail Adel A, Al-Sayari SA, Bahnemann D, Afanasev D, Emeline AV. Mesoporous TiO_2 nanocrystals as efficient photocatalysts: Impact of calcination temperature and phase transformation on photocatalytic performance. Chemical Engineering Journal. 2015;**264**:417-424. DOI: 10.1016/j.cej.2014.11.075

[55] Mutuma BK, Shao GN, Kim WD, Kim HT. Sol-gel synthesis of mesoporous anatase-brookite and anatase-brookite-rutile TiO_2 nanoparticles and their photocatalytic properties. Journal of Colloid and Interface Science. 2015;**442**:1-7. DOI: 10.1016/j.jcis.2014.11.060

[56] Siwińska-Stefańska K, Zdarta J, Paukszta D, Jesionowski T. The influence of addition of a catalyst and chelating agent on the properties of titanium dioxide synthesized via the sol-gel method. Journal of Sol-Gel Science and Technology. 2015;**75**(2):264-278. DOI 10.1007/s10971-015-3696-2

[57] Ingo GM, Riccucci C, Bultrini G, Dirè S, Chiozzini G. Thermal and microchemical characterisation of sol-gel SiO_2, TiO_2 and $xSiO_2$-$(1-x)TiO_2$ ceramic materials. Journal of Thermal Analysis and Calorimetry. 2001;**66**(1):37-46. DOI: 10.1023/A:1012471112566

[58] Siwińska-Stefańska K, Paukszta D, Piasecki A, Jesionowki T. Synthesis and physicochemical characteristics of titanium dioxide doped with selected metals. Physicochemical Problems of Mineral Processing. 2014;**50**(1):265-276. DOI: 10.5277/ppmp140122

[59] Fan M, Hu S, Ren B, Wang J, Jing X. Synthesis of nanocomposite TiO_2/ZrO_2 prepared by different templates and photocatalytic properties for the photodegradation of Rhodamine B. Powder Technology. 2013;**235**:27-32. DOI: 10.1016/j.powtec.2012.09.042

[60] Shao GN, Imran SM, Jeon SJ, Engole M, Abbas N, Salman Haider M, Kang SJ, Kim HT. Sol-gel synthesis of photoactive zirconia-titania from metal salts and investigation of their photocatalytic properties in the photodegradation of methylene blue. Powder Technology. 2014;**258**:9-109. DOI: 10.1016/j.powtec.2014.03.024

[61] Kraleva E, Ehrich H. Synthesis, characterization and activity of Co and Ni catalysts supported on AlMe (Me = Zn, Zr, Ti) mixed oxides. Journal of Sol-Gel Science and Technology. 2012;**64**(3):619-629. DOI: 10.1007/s10971-012-2893-5

[62] Kraleva E, Saladino ML, Matassa R, Caponetti E, Enzo S, Spojakina A. Phase formation in mixed TiO_2-ZrO_2 oxides prepared by sol-gel method. Journal of Structural Chemistry. 2011;**52**(2):330-339. DOI: 10.1134/S0022476611020132

[63] Byrappa K, Yoshimura M. Handbook of hydrothermal technology. 1st ed. New York: William Andrew & Sons; 2001. 893 p.

[64] Holzinger M, Maier J, Sitte W. Fast CO_2-selective potentiometric sensor with open reference electrode. Solid State Ionics. 1996;**86-88**:1055-1062. DOI: 10.1016/0167-2738(96)00250-0

[65] Chae SY, Park MK, Lee SK, Kim TY, Kim SK, Lee WI. Preparation of size-controlled TiO_2 nanoparticles and derivation of optically transparent photocatalytic films. Chemistry of Materials. 2003;**15**(17):3326-3331. DOI: 10.1021/cm030171d

[66] Zhang YX, Li GH, Jin YX, Zhang Y, Zhang J, Zhang LD. Hydrothermal synthesis and photoluminescence of TiO_2 nanowires. Chemical Physics Letters. 2002;**365**(3-4):300-304. DOI: 10.1016/S0009-2614(02)01499-9

[67] Caillot T, Salama Z, Chantur N, Cadete Santos Aires FT, Bennici S, Auroux A. Hydrothermal synthesis and characterization of zirconia based catalysts. Journal of Solid State Chemistry. 2013;**203**:79-85. DOI: 10.1016/j.jssc.2013.04.005

[68] Hirano M, Nakahara C, Ota K, Tanaike O, Inagaki M. Photoactivity and phase stability of ZrO_2-doped anatase-type TiO_2 directly formed as nanometer-sized particles by hydrolysis under hydrothermal conditions. Journal of Solid State Chemistry. 2003;**70**(1): 39-47. DOI: 10.1016/s0022-4596(02)00013-0

[69] Kim CS, Moon BK, Park JH, Choi BC, Seo HJ. Solvothermal synthesis of nanocrystalline TiO_2 in toluene with surfactant. Journal of Crystal Growth. 2003;**257**(3-4):309-315. DOI: 10.1016/S0022-0248(03)01468-4

[70] Wen B, Liu C, Liu Y. Solvothermal synthesis of ultralong single-crystalline TiO_2 nanowires. New Journal of Chemistry. 2005;**29**:969-971. DOI: 10.1039/B502604K

[71] Zhu L, Liu K, Li H, Sun Y, Qiu M. Solvothermal synthesis of mesoporous TiO_2 microspheres and their excellent photocatalytic performance under simulated sunlight irradiation. Solid State Sciences. 2013;**20**:8-14. DOI: 10.1016/j.solidstatesciences. 2013.02.026

[72] Yang HG, Liu G, Qiao SZ, Sun CH, Jin YG, Smith C, Zou J, Cheng HM, Lu GQ. Solvothermal synthesis and photoreactivity of anatase TiO_2 nanosheets with dominant {001} facets. Journal of the American Chemical Society. 2009;**131**(11):4078-4083. DOI: 10.1021/ja808790p

[73] Oshima K, Nakashima K, Ueno S, Wada S. Synthesis of titanium dioxide nanoparticles by solvothermal method with polymer gel. Transactions of the Materials Research Society of Japan. 2014;**39**(4):451-454. DOI: 10.14723/tmrsj.39.451

[74] Supphasrirongjaroen P, Praserthdam P, Mekasuwandumrong O, Panpranot J, Impact of Si and Zr addition on the surface defect and photocatalytic activity of the nanocrystalline TiO_2 synthesized by the solvothermal method. Ceramics International. 2010;**36**(4):1439-1446. DOI: 10.1016/j.ceramint.2010.02.001

[75] Herrmann JM. Fundamentals and misconceptions in photocatalysis. Journal of Photochemistry and Photobiology. 2010;**216**(2-3):85-93. DOI: 10.1016/j.jphotochem.2010.05.015

[76] Lacombe S, Keller N. Photocatalysis: Fundamentals and applications in JEP 2011. Environmental Science and Pollution Research. 2012;**19**(9):3651-365. DOI: 10.1007/s11356-012-1040-8

[77] Langford C. Photocatalysis—A special issue on a unique hybrid area of catalysis. Catalysts. 2012;**2**(3):327-329. DOI: 10.3390/catal2030327

[78] Fujishima A, Rao TN, Try DA. Titanium dioxide photocatalysis. Journal of Photochemistry and Photobiology C. 2000;**1**(1):1-21. DOI: 10.1016/S1389-5567(00)00002-2

[79] Ray M, Ajay K. Heterogeneous photocatalysis in environmental remediation. Developments in Chemical Engineering and Mineral Processing. 2000;**8**:505-550. DOI: 10.1002/apj.5500080507

[80] Ibhadon AO, Fitzpatrick P. Heterogeneous photocatalysis: Recent advances and applications. Catalysts. 2013;**3**(1)189-218. DOI: 10.3390/catal3010189

[81] Friedmanna D, Mendive C, Bahnemann D. TiO_2 for water treatment: Parameters affecting the kinetics and mechanisms of photocatalysis. Applied Catalysis B. 2010;**99**(3-4):398-406, DOI: 10.1016/j.apcatb.2010.05.014

[82] Teoh WY, Amal R, Scott J. Progress in heterogenours photocatalysis: From classical radical chemistry to engineering nanomaterials and solar reactors. Journal of Physical Chemistry Letters. 2012;**3**(5):629-639. DOI: 10.1021/jz3000646

[83] Carp O, Huisman CL, Reller A. Photoinduced reactivity of titanium dioxide. Progress in Solid State Chemistry. 2004;**32**(1-2):33-177. DOI: 10.1016/j.progsolidstchem.2004.08.001

[84] Kosowska B, Mozia S, Morawski AW, Grzmil B, Janus M, Kałucki K. The preparation of TiO_2-nitrogen doped by calcination of $TiO_2 \cdot xH_2O$ under ammonia atmosphere for visiblbe light photocatalysis. Solar Energy Materials and Solar Cells. 2005;**88**(3):269-280. DOI: 10.1016/j.solmat.2004.11.001

[85] Janus M, Inagaki M, Tryba B, Toyoda M, Morawski AW. Carbon-modified TiO_2 photocatalyst by ethanol carbonisation. Applied Catalysis B. 2006:**63**(3-4):272-276. DOI: 10.1016/j.apcatb.2005.10.005

[86] Inagaki M, Nonaka R, Tryba B, Morawski AW. Dependence of photocatalytic activity of anatase powders on their crystallinity. Chemosphere. 2006;**64**(3)437-445. DOI: 10.1016/j.chemosphere.2005.11.052

[87] Li YF, Liu ZP. Particle size, shape and activity for photocatalysis on titania anatase nanoparticles in aqueous surroundings. Journal of the American Chemical Society. 2011;**133**(39):15743-15752. DOI: 10.1021/ja206153v

[88] Tanaka K, Capule MFV, Hisanaga T. Effect of crystallinity of TiO_2 on its photocatalytic action. Chemical Physics Letters. 1991;**187**(1-2):73-76. DOI: 10.1016/0009-2614(91)90486-S

[89] Kumar KNP, Keizer K, Burrgraaf AJ. Textural evolution and phase transformation in titania membranes: Part 1.—Unsupported membranes. Journal of Materials Chemistry. 1993;**3**(11):1141-1149. DOI: 10.1039/JM9930301141

[90] Linsebigler AL, Lu G, Yates J. Photocatalysis on TiO_2 surfaces: Principles, mechanisms, and selected results. Chemical Reviews. 1995;**95**(3):735-758. DOI: 10.1021/cr00035a013

[91] Hoffmann MR, Martin ST, Choi W, Bahnemann DW. Environmental applications of semiconductor photocatalysis. Chemical Reviews. 1995;**95**(1):69-96. DOI: 10.1021/cr00033a004

[92] Hermann JM. Heterogeneous photocatalysis: Fundamentals and applications to the removal of various types of aqueous pollutants. Catalysis Today. 1999;**53**(1):115-129. DOI: 10.1016/S0920-5861(99)00107-8

[93] Lam RCW, Leung MKH, Leung DYC, Vrijmoed LLP, Yam WC, Ng SP. Visible-light-assisted photocatalytic degradation of gaseous formaldehyde by parallel-plate reactor coated with Cr ion-implanted TiO_2 thin film. Solar Energy Materials and Solar Cells. 2007;**91**(1):54-61. DOI: 10.1016/j.solmat.2006.07.004

[94] Venkatachalam N, Palanichamy M, Arabindoo B, Murugesan V. Enhanced photocatalytic degradation of 4-chlorophenol by Zr^{4+} doped nano TiO_2. Journal of Molecular Catalysis A. 2007;**266**(1-2):158-165. DOI: 10.1016/j.molcata.2006.10.051

[95] Di Paola A, Garcia-Lopez E, Ikeda S, Marci G, Ohtani B, Palmisano L. Photocatalytic degradation of organic compounds in aqueous systems by transition metal doped polycrystalline TiO_2. Catalysis Today. 2002;**75**(1-4)87-93. DOI: 10.1016/S0920-5861(02)00048-2

[96] Hagfeldt A, Grätzel M. Light-induced redox reactions in nanocrystalline systems. Chemical Reviews. 1995;**95**:49-68. DOI: 10.1021/cr00033a003

[97] Chatterjee D, Mahata A. Demineralization of organic pollutants on the dye modified TiO_2 semiconductor particulate system using visible light. Applied Catalysis B. 2001;**33**(2):119-125. DOI: 10.1016/S0926-3373(01)00170-9

[98] Chatterjee D, Dasgupta S. Visible light induced photocatalytic degradation of organic pollutants. Journal of Photochemistry and Photobiology C. 2005;**6**(2-3):186-205. DOI: 10.1016/j.jphotochemrev.2005.09.001

[99] Fang X, Zhang Z, Chen Q, Ji H. Dependence of nitrogen doping on TiO_2 precursor annealed under NH_3 flow. Journal of Solid State Chemistry. 2007;**180**(4):1325-1332. DOI: 10.1016/j.jssc.2007.02.010

[100] Oropeza FE, Harmer J, Egdell RG, Palgrave RG. A critical evaluation of the mode of incorporation of nitrogen in doped anatase photocatalysts. Physical Chemistry Chemical Physics. 2010;**12**:960-969. DOI: 10.1039/B914733K

[101] Irie H, Watanabe Y, Hashimoto K. Carbon-doped anatase TiO_2 powders as a visible-light sensitive photocatalyst. Chemical Letters. 2003;**32**(8):772-773. DOI: 10.1246/cl.2003.772

[102] Sakthivel S, Kisch H. Daylight photocatalysis by carbon-modified titanium dioxide. Angewandte Chemie International Edition. 2003;**42**(40):4908-4911. DOI: 10.1002/anie.200351577

[103] Kociołek-Balawejder E, Szymczyk M. Titanium dioxide as pigment and photocatalyst. Przemysł Chemiczny. 2007;**86**(12):1179-1188

[104] Hirano M, Ota K, Inagaki M, Iwata H. Hydrothermal synthesis of TiO_2/SiO_2 composite nanoparticles and their photocatalytic performances. Journal of the Ceramic Society of Japan. 2004;**112**(1303):143-148.

[105] Ren J, Li Z, Liu S, Xing Y, Xie K. Silica-titania mixed oxides: Si-O-Ti connectivity, coordination of titanium, and surface acidic properties. Catalysis Letters. 2008;**124**(3-4):185-194. DOI: 10.1007/s10562-008-9500-y

[106] Ambrus Z, Balázs N, Alapi T, Wittmann G, Sipos P, Dombi A, Mogyorósi K. Synthesis, structure and photocatalytic properties of Fe(III)-doped TiO_2 prepared from $TiCl_3$. Applied Catalysis B: Environmental 2008;**81**(1-2):27-37. DOI: 10.1016/j.apcatb.2007.11.041

[107] Sathasivam S, Bhachu DS, Lu Y, Chadwick N, Althabaiti SA, Alyoubi AO, Basahel SN, Carmalt CJ, Parkin IP. Tungsten doped TiO_2 with enhanced photocatalytic and

optoelectrical properties via aerosol assisted chemical vapor deposition. Scientific Reports. 2015;**5**:1-10 DOI: 10.1038/srep10952

[108] Hwang YJ, Yang S, Lee H. Surface analysis of N-doped TiO_2 nanorods and their enhanced photocatalytic oxidation activity. Applied Catalysis B. 2017;**204**:209-215. DOI: 10.1016/j.apcatb.2016.11.038

[109] Bakar SA, Byzynski G, Ribeiro C. Synergistic effect on the photocatalytic activity of N-doped TiO_2 nanorods synthesised by novel route with exposed (110) facet. Journal of Alloys and Compounds. 2016;**666**:38-49. DOI: 10.1016/j.jallcom.2016.01.112

[110] Szatmáry L, Bakardjieva S, Šubrt J, Bezdička P, Jirkovskỳ J, Bastl Z, Brezová V, Korenko M. Sulphur doped nanoparticles of TiO_2. Catalysis Today. 2011:**161**(1):23-28. DOI: 10.1016/j.cattod.2010.11.082

[111] Rockafellow EM, Stewart LK, Jenks WS. Is sulfur-doped TiO_2 an effective visible light photocatalyst for remediation?. Applied Catalysis B. 2009;**91**(1-2):554-562. DOI: 10.1016/j.apcatb.2009.06.027

[112] Cheng P, Wang Y, Xu L, Sun P, Su Z, Jin F, Liu F, Sun Y, Lu G. High specific surface area urchin-like hierarchical ZnO-TiO_2 architectures: Hydrothermal synthesis and photocatalytic properties. Materials Letters. 2016;**175**:52-55. DOI: 10.1016/j.matlet.2016.03.120

[113] Zhou W, Liu K, Fu H, Pan K, Zhang L, Wang L, Sun C. Multi-modal mesoporous TiO_2-ZrO_2 composites with high photocatalytic activity and hydriophilicity. Nanotechnology. 2008;**19**(3):1-7. DOI: 10.1088/0957-4484/19/03/035610

[114] Yan W, He F, Gai S, Gao P, Chen Y, Yang P. A novel 3D structured reduced graphene oxide/TiO_2 composite: Synthesis and photocatalytic performance. Journal of Materials Chemistry A. 2014;**2**:3605-3612. DOI: 10.1039/C3TA14718E

[115] Thomas RT, Rasheed PA, Sandhyarani N. Synthesis of nanotitania decorated few-layer graphene for enhanced visible light driven photocatalysis. Journal of Colloid and Interface Science. 2014;**428**:214-221. DOI: 10.1016/j.jcis.2014.04.054

[116] Gupta SM, Tripathi M. A review of TiO_2 nanoparticles. Chinese Science Bulletin. 2011;**56**(16):1639-1657. DOI: 10.1007/s11434-011-4476-1

[117] Ismail AA, Bahnemann DW. Mesoporous titania photocatalysts: Preparation, characterization and reaction mechanisms. Journal of Materials Chemistry. 2011;**21**(32):11686-11707. DOI: 10.1039/C1JM10407A

[118] Choi WY, Termin A, Hoffmann MR. The role of metal ion dopants in quantum-sized TiO_2: Correlation between photoreactivity and charge carrier recombination dynamics. The Journal of Physical Chemistry. 1994;**98**(51):13669-13679. DOI: 10.1021/j100102a038

[119] Litter MI. Heterogeneous photocatalysis: Transition metal ions in photocatalytic systems. Applied Catalysis B. 1999;**23**(2-3):89-114. DOI: 10.1016/S0926-3373(99)00069-7

[120] Tayade RJ, Kulkarni RG, Jasra RV. Transition metal ion impregnated mesoporous TiO_2 for photocatalytic degradation of organic contaminants in water. Industrial & Engineering Chemistry Research. 2006;**45**(15):5231-5238. DOI: 10.1021/ie051362o

[121] Khan, M, Cao, W. Preparation of Y-doped TiO_2 by hydrothermal method and investigation of its visible light photocatalytic activity by the degradation of methylene blue. Journal of Molecular Catalysis A. 2013;**376**:71-77. DOI: 10.1016/j.molcata.2013.04.009

[122] Golubović A, Tomić N, Finčur N, Abramović B, Veljković I, Zdravković J, Grujić-Brojčin M, Babić B, Stojadinović B, Šćepanović M. Synthesis of pure and La-doped anatase nanopowders by sol-gel and hydrothermal methods and their efficiency in photocatalytic degradation of alprazolam. Ceramics International. 2014;**40**(8):13409-13418. DOI: 10.1016/j.ceramint.2014.05.060

[123] Kim DH, Choi DK, Kim SJ, Lee KS. The effect of phase type on photocatalytic activity in transition metal doped TiO_2 nanoparticles. Catalysis Communications. 2008;**9**(5):654-657. DOI: 10.1016/j.catcom.2007.07.017

[124] Jing LQ, Sun XJ, Xin BF, Wang BQ, Cai WM, Fu HG. The preparation and characterization of La doped TiO_2 nanoparticles and their photocatalytic activity. Journal of Solid State Chemistry. 2004;**177**(10):3375-3382. DOI: 10.1016/j.jssc.2004.05.064

[125] Mozia S, Heciak A, Morawski AW. Preparation of Fe-modified photocatalysts and their application for generation of useful hydrocarbons during photocatalytic decomposition of acetic acid. Journal of Photochemistry and Photobiology A. 2010;**216**(2-3):275-282. DOI: 10.1016/j.jphotochem.2010.09.016

[126] Zhou M, Yu J, Cheng B. Effects of Fe-doping on the photocatalytic activity of mesoporous TiO_2 powders prepared by an ultrasonic method. Journal of Hazardous Materials. 2006;**137**(3):1838-1847. DOI: 10.1016/j.jhazmat.2006.05.028

[127] Hung WC, Chen YC, Chu H, Tseng TK. Synthesis and characterization of TiO_2 and Fe/TiO_2 nanoparticles and their performance for photocatalytic degradation of 1,2-dichloroethane. Applied Surface Science. 2008;**255**(5):2205-2213. DOI: 10.1016/j.apsusc.2008.07.079

[128] Khan MA, Woo SI, Yang OB. Hydrothermally stabilized Fe(III) doped titania active under visible light for water splitting reaction. International Journal of Hydrogen Energy. 2008:**33**(20):5345-5351. DOI: 10.1016/j.ijhydene.2008.07.119

[129] Litter MI, Navío JA. Photocatalytic properties of iron-doped titania semiconductors. Journal of Photochemistry and Photobiology A. 1996;**98**(3):171-181. DOI: 10.1016/1010-6030(96)04343-2

[130] Hajjaji A, Atyaoui A, Trabelsi K, Amlouk M, Bousselmi L, Bessais B, Khakani MAE, Gaidi M, Cr-doped TiO_2 thin films prepared by means of a magnetron co-sputtering process: Photocatalytic application. American Journal of Analytical Chemistry. 2014;**5**(8):473-482. DOI: 10.4236/ajac.2014.58056

[131] Kafizas A, Parkin IP. Combinatorial atmospheric pressure chemical vapor deposition (cAPCVD): A route to functional property optimization. Journal of the American Chemical Society. 2011;**133**(50):20458-20467. DOI: 10.1021/ja208633g

[132] Treschev SY, Chou PW, Tseng TH, Wang JB, Perevedentseva EV, Cheng CL. Photoactivities of the visible light-activated mixedphase carbon-containing titanium dioxide: The effect of carbon incorporation. Applied Catalysis B. 2008;**79**(1):8-16. DOI: 10.1016/j.apcatb.2007.09.046

[133] Lettmann C, Hildebrand K, Kisch H, Macyk W, Maier W. Visible light photodegradation of 4-chlorophenol with a coke-containing titanium dioxide photocatalyst. Applied Catalysis B. 2001;**32**(4):215-222. DOI: 10.1016/S0926-3373(01)00141-2

[134] Tojo S, Tachikawa T, Fujitsuka M, Majima T. Iodine-doped TiO_2 photocatalysts: Correlation between band structure and mechanism. The Journal of Physical Chemistry C. 2008;**112**(38):14948-14954. DOI: 10.1021/jp804985f

[135] Choi H, Antoniou MG, Pelaez M, Delacruz AA, Shoemaker OA, Dionysiou DD. Mesoporous nitrogen-doped TiO_2 for the photocatalytic destruction of the cyanobacterial toxin microcystin-LR under visible light irradiation. Environmental Science & Technology. 2007;**41**(21):7530-7535. DOI: 10.1021/es0709122

[136] Fang J, Wang F, Qian K, Bao H, Jiang Z, Huang W. Bifunctional N-doped mesoporous TiO_2 photocatalysts. The Journal of Physical Chemistry C. 2008;**112**(46):18150-18156. DOI: 10.1021/jp805926b

[137] Cong Y, Zhang J, Chen F, Anpo M. Preparation, photocatalytic activity, and mechanism of nano-TiO_2 Co-doped with nitrogen and iron(III). The Journal of Physical Chemistry C. 2007;**111**(28):6976-6982. DOI: 10.1021/jp0727493

[138] Liu H, Su Y, Hu H, Cao W, Chen Z. An ionic liquid route to prepare mesoporous ZrO_2-TiO_2 nanocomposites and study on their photocatalytic activities. Advanced Powder Technology. 2013;**24**(3):683-688. DOI: 10.1016/j.apt.2012.12.007

[139] Tian J, Chen L, Dai J, Wang X, Yin Y, Wu P. Preparation and characterization of TiO_2, ZnO, and TiO_2/ZnO nanofilms via sol-gel process. Ceramics International. 2009;**35**(6):2261-2270. DOI: 10.1016/j.ceramint.2008.12.010

[140] Cheng P, Wang Y, Xu L, Sun P, Su Z, Jin F, Liu F, Sun Y, Lu G. High specific surface area urchin-like hierarchikal ZnO-TiO_2 architectures: Hydrothermal synthesis and photocatalytic properties. Material Letters. 2016;**175**:52-55. DOI:10.1016/j.matlet.2016.03.120

[141] Qiu J., Zhang P, Ling M, Li S, Liu P, Zhao H, Zhang S. Photocatalytic synthesis of TiO_2 and reduced graphene oxide nanocomposite for lithium ion battery. ACS Applied Materials & Interfaces. 2012;**4**(7):3636-3642. DOI: 10.1021/am300722d

[142] Ni Y, Wang W, Huang W, Lu C, Xu Z. Graphene strongly wrapped TiO_2 for high-reactive photocatalyst: A new sight for significant application of graphene. Journal of Colloid and Interface Science. 2014;**428**:162-169. DOI: 10.1016/j.jcis.2014.04.022

[143] Tang H, Zhang J, Zhang YJ, Xiong QQ, Tong YY, Li Y, Wang XL, Gu CD, Tu JP. Porous reduced graphene oxide sheet wrapped silicon composite fabricated by steam etching for lithium-ion battery application. Journal of Power Sources. 2015;**286**:431-437. DOI: 10.1016/j.jpowsour.2015.03.185

[144] Wang X, Wang Y, Yang L, Wang K, Lou X, Cai B. Template-free synthesis of homogeneous yolk-shell TiO_2 hierarchical microspheres for high performance lithium ion batteries. Journal of Power Sources. 2014;**262**:72-78. DOI: 10.1016/j.jpowsour.2014.03.081

[145] Wang X, Xi M, Wang X, Fong H, Zhu Z. Flexible composite felt of electrospun TiO_2 and SiO_2 nanofibers infused with TiO_2 nanoparticles for lithium ion battery anode. Electrochimica Acta. 2016;**190**:811-816. DOI: 10.1016/j.electacta.2015.12.123

[146] Tong X, Zeng M, Li J, Li F. UV-assisted synthesis of surface modified mesoporous TiO_2/G microspheres and its electrochemical performances in lithium ion batteries. Applied Surface Science. 2017;**392**:897-903. DOI: 10.1016/j.apsusc.2016.09.094

[147] Choi DW, Choy K-L. Novel nanostructured SiO_2/ZrO_2 based electrodes with enhanced electrochemical performance for lithium-ion batteries. Electrochimica Acta. 2016;**218**:47-53. DOI: 10.1016/j.electacta.2016.08.116

[148] Armstrong MJ, Burke DM, Gabriel T, O'Regan C, O'Dwyer C, Petkovac N, Holmes JD. Carbon nanocage supported synthesis of V_2O_5 nanorods and V_2O_5/TiO_2 nanocomposites for Li-ion batteries. Journal of Materials Chemistry A. 2013;**1**(40):12568-12578. DOI: 10.1039/C3TA12652H

[149] Madian M, Giebeler L, Klose M, Jaumann T, Uhlemann M, Gebert A, Oswald S, Ismail N, Eychmüller A, Eckert J. Self-organized TiO_2/CoO nanotubes as potential anode materials for lithium ion batteries. ACS Sustainable Chemistry and Engineering. 2015;**3**(5):909-919. DOI: 10.1021/acssuschemeng.5b00026

[150] Ma D, Dou P, Yu X, Yang H, Meng H, Sun Y, Zheng J, Xu X. Novel hollow SnO_2 nanosphere@TiO_2 yolk-shell hierarchical nanospheres as anode material for high-performance lithium-ion batteries. Materials Letters. 2015;**157**:228-230. DOI: 10.1016/j.matlet.2015.05.121

[151] Lü X, Yang W, Quan Z, Lin T, Bai L, Wang L, Huang F, Zhao Y. Enhanced electron transport in Nb-doped TiO_2 nanoparticles via pressure-induced phase transitions. Journal of the American Chemical Society. 2014;**136**(1):419-426. DOI: 10.1021/ja410810w

[152] Das SK, Gnanavel M, Patel MUM, Shivakumara C, Bhattacharyya AJ. Anamolously high lithium storage in mesoporous nanoparticulate aggregation of Fe^{3+} doped anatase titania. Journal of the Electrochemical Society. 2011;**158**(12):A1290-A1297. DOI: 10.1149/2.029112jes

[153] Kubiak P, Geserick J, Hüsing N, Wohlfahrt-Mehrens M. Electrochemical performance of mesoporous TiO_2 anatase. Journal of Power Sources. 2008;**175**:510-516. DOI: 10.1016/j.jpowsour.2007.09.044

[154] Mancini M, Kubiak P, Geserick J, Marassi R, Hüsing N, Wohlfahrt-Mehrens M. Mesoporous anatase TiO_2 composite electrodes: Electrochemical characterization and high rate performances. Journal of Power Sources. 2009;**189**(1):585-589. DOI: 10.1016/j.jpowsour.2008.10.050

[155] Kubiak P, Pfanzelt M, Geserick J, Hörmann U, Hüsing N, Kaiser U, Wohlfahrt-Mehrens M. Electrochemical evaluation of rutile TiO_2 nanoparticles as negative electrode for Li-ion batteries. Journal of Power Sources. 2009;**194**:1099-1104. DOI: 10.1016/j.jpowsour.2009.06.021

[156] Jung H-G, Oh SW, Ce J, Jayaprakash N, Sun Y-K. Mesoporous TiO_2 nano networks: Anode for high power lithium battery applications. Electrochemistry Communications. 2009;**11**(4);756-759. DOI: 10.1016/j.elecom.2009.01.030

[157] Zhang F, Zhang Y, Song S, Zhang H. Superior electrode performance of mesoporous hollow TiO_2 microspheres through efficient hierarchical nanostructures. Journal of Power Sources. 2001;**196**(20):8618-8624. DOI: 10.1016/j.jpowsour.2011.06.006

[158] Li Y, Wang Z, Lv X-J. N-doped TiO_2 nanotubes/N-doped graphene nanosheets composites as high performance anode materials in lithium-ion battery. Journal of Materials Chemistry A. 2014;**2**(37):15473-15479. DOI: 10.1039/C4TA02890B

[159] Opra DP, Gnedenkov SV, Sokolov AA, Zheleznov VV, Voit EI, Sushkov YV, Sinebryukhov SL. Enhancing the reversible capacity of nanostructured TiO_2(anatase) by Zr-doping using a sol-gel template method. Scripta Materialia. 2015;**107**:136-139. DOI: 10.1016/j.scriptamat.2015.06.004

[160] Gao L, Li S, Huang D, Shen Y, Wang M. ZnO decorated TiO_2 nanosheet composites for lithium ion battery. Electrochimica Acta. 2015;**182**:529-536. DOI: 10.1016/j.electacta.2015.09.108

[161] Siwińska-Stefańska K, Kurc B. A novel composite TiO_2-SiO_2-ZrO_2 oxide system as a high-performance anode material for lithium-ion batteries. Journal of the Electrochemical Society. 2017;**164**(4):A728-A734. DOI: 10.1149/2.0911704jes

[162] Zhu, Q, Hu, H, Li, G, Zhu, C, Yu, Y. TiO_2 nanotube arrays grafted with MnO_2 nanosheets as high-performance anode for lithium ion battery. Electrochimica Acta. 2015;**156**:252-260. DOI: 10.1016/j.electacta.2015.01.023

[163] Yun YS, Le V-D, Kim H, Chang S-J, Baek SJ, Park S, Kim BH, Kim Y-H, Kang K, Jin H-J. Effects of sulfur doping on graphene-based nanosheets for use as anode materials in lithium-ion batteries. Journal of Power Sources. 2014;**262**:79-85. DOI: 10.1016/j.jpowsour.2014.03.084

[164] Di Lupo F, Tuel A, Mendez V, Francia C, Meligrana G, Bodoardo S, Gerbaldi C. Mesoporous TiO_2 nanocrystals produced by a fast hydrolytic process as high-rate long-lasting Li-ion battery anodes. Acta Materialia. 2014;**69**:60-67. DOI: 10.1016/j.actamat.2014.01.057

[165] Xiu Z, Hao X, Wu Y, Lu Q, Liu S. Graphene-bonded and -encapsulated mesoporous TiO_2 microspheres as a high-performance anode material for lithium ion batteries. Journal of Power Sources. 2015;**287**:334-340. DOI: 10.1016/j.jpowsour.2015.04.086

[166] Li D, Shi D, Liu Z, Liu H, Guo Z. TiO_2 nanoparticles on nitrogen-doped graphene as anode material for lithium ion batteries. Journal of Nanoparticle Research. 2013;**15**(5):1674-1683. DOI: 10.1007/s11051-013-1674-6

[167] Qiu J, Lai C, Wang Y, Li S, Zhang S. Resilient mesoporous TiO_2/graphene nanocomposite for high rate performance lithium-ion batteries. Chemical Engineering Journal. 2014;**256**:247-254. DOI: 10.1016/j.cej.2014.06.116

[168] Zhang JJ, Wei Z, Huang T, Liu Z-L, Yu A-S. Carbon coated TiO_2-SiO_2 nanocomposites with high grain boundary density as anode materials for lithium-ion batteries. Journal of Materials Chemistry A. 2013;**1**(25):7360-7369. DOI: 10.1039/c3ta11137g

[169] Siwińska-Stefańska K, Kurc B. Preparation and application of a titanium dioxide/graphene oxide anode material for lithium-ion batteries. Journal of Power Sources. 2015;**299**:286-292. DOI: 10.1016/j.jpowsour.2015.09.017

[170] Wang J, Ran R, Tade MO, Shao Z. Self-assembled mesoporous TiO_2/carbon nanotube composite with a three-dimensional conducting nanonetwork as a high-rate anode material for lithium-ion battery. Journal of Power Sources. 2014;**254**:18-28. DOI: 10.1016/j.jpowsour.2013.12.090